Discrete maximum principle preserving scheme for 1-d nonlocal to local diffusion problem: development, analysis, simulation, and application

by

Amanda Gute

A thesis submitted to the faculty of
The University of North Carolina at Charlotte
in partial fulfillment of the requirements
for the degree of Doctor of Philosophy in
Applied Mathematics

Charlotte

2024

Approved by:

Dr. Ronald E. Smelser

Dr. Duan Chen

Dr. Loc Nguyen

Dr. Kevin McGoff

Dr. Bei-Tseng Chu

ABSTRACT

AMANDA GUTE. Discrete maximum principle preserving scheme for 1-d nonlocal to local diffusion problem: development, analysis, simulation, and application. (Under the direction of DR. RONALD E. SMELSER)

Diffusion is a scientific phenomena that can be modeled by partial differential equations. In this paper we first explore the development of equations for local, nonlocal, and quasi-nonlocal diffusion. Methods of finding solutions will be discussed as well as the properties of each diffusion model type. These properties include satisfying the maximum principle and demonstrating the well-posedness of each model which is through the solutions existence, uniqueness, and stability.

Also in a recent paper, a quasi-nonlocal coupling method was introduced to seamlessly bridge a nonlocal diffusion model with the classical local diffusion counterpart in a one-dimensional space. The proposed coupling framework removes interfacial inconsistency, preserves the balance of fluxes, and satisfies the maximum principle of the diffusion problem. However, the numerical scheme proposed in that paper does not maintain all of these properties on a discrete level. We resolve this issue by proposing a new finite difference scheme that ensures the balance of fluxes and the discrete maximum principle. We rigorously prove these results and provide the stability and convergence analyses accordingly. In addition, we provide the Courant-Friedrichs-Lewy (CFL) condition for the new scheme and test a series of benchmark examples which confirm the theoretical findings.

ACKNOWLEDGEMENTS

I would like to thank my advisor Dr. Ron Smelser, Co-Chair Dr. Duan Chen, and committee members Dr. Loc Nguyen, Dr. Kevin McGoff, and Dr. Bei-Tseng Chu, with special thanks to Dr. Oleg Safranov, Dr. Hae-Soo Oh, Dr. Shaozhoung Deng, Dr. Mohammad Kazemi, and Dr. Taufiquar Khan.

I would also like to acknowledge the financial support I received through research funding provided by Dr. X. Li who is supported by an NSF CAREER award: DMS-1847770 and the University of North Carolina at Charlotte Faculty Research Grant. Also other funding was provided by a Graduate School Summer Fellowship Grant (GSSF), Graduate Assistant Support Plan (GASP), and various travel grants from American Mathematical Society (AMS), University of North Carolina at Charlotte, Graduate and Professional Student Government (GPSG), and the University of North Carolina at Charlotte Mathematics Department.

Finally I would like to thank my family for their support through a very long academic journey, my kids for sacrificing time with their mom, and most of all my husband who has sat next to me and supported me in school since the first grade.

TABLE OF CONTENTS v

LIST OF TABLES vii

LIST OF FIGURES viii

CHAPTER 1: INTRODUCTION 1

CHAPTER 2: LOCAL DIFFUSION 3

2.1. Deriving the Local Diffusion Model 3

2.2. Properties of Local Diffusion 8

2.3. Local Diffusion Conclusion 14

CHAPTER 3: NONLOCAL DIFFUSION 15

3.1. Deriving the Nonlocal Diffusion Model 16

3.2. Properties of Nonlocal Diffusion 21

3.3. Nonlocal Diffusion Conclusion 27

CHAPTER 4: COUPLING NONLOCAL AND LOCAL DIFFUSION 28

CHAPTER 5: FINITE DIFFERENCE SCHEME FOR QNL COUPLING 35

5.1. Discretized Quasi-Nonlocal Coupling 37

5.2. Consistency of the Discretized Quasi-Nonlocal Operator 41

5.3. Stability of the Discretized Quasi-nonlocal Operator 47

5.4. Convergence of Discretized Quasi-nonlocal Operator 55

5.5. Study of the Courant-Friedricks-Lewy (CFL) Condiditon 57

5.6. Numerical Examples 61

5.7. New Finite Difference Scheme Conclusion 64

CHAPTER 6: DEVELOPMENT OF COEFFICIENT MATRICIES AND ADDITION OF NEUMANN AND ROBIN BOUNDARY CONDITIONS 65

6.1. Derivation of the Numerical Operator from the Continuous Operator and development of Coefficient Matrix for Dirichlet Boundary Conditions 67

6.2. Coefficient Matrix with Neumann Boundary Conditions and Numerical Example 74

6.3. Coefficient Matrix with Robin Boundary Conditions and Numerical Example 78

6.4. Boundary Conditions Conclusion 81

REFERENCES 82

TABLE 5.1: $L^{\infty}_{\Omega\times[0,T]}$ differences between the local continuous solution u^{ℓ} and discrete solution $u^{qnl}_{\delta,\Delta x}$. We fix $\delta = 3\Delta x$, and the kernel is $\gamma_{\delta}(s) = \frac{3}{\delta^3}\chi_{[-\delta,\delta]}(s)$. The termination time $T = 1$ and $\Delta t = 0.2\Delta x$. 62

TABLE 5.2: $L^{\infty}_{\Omega\times[0,T]}$ differences between the local continuous solution u^{ℓ} and two discrete solutions $u^{qnl}_{\delta,\Delta x}$, $\tilde{u}^{qnl}_{\delta,\Delta x}$ using the FDM schemes (5.6) and (5.8), respectively. We fix $\delta = 3\Delta x$, and the kernel is $\gamma_{\delta}(s) = \frac{3}{\delta^3}$. The termination time is $T = 1$ and $\Delta t = 0.2\Delta x$. 63

TABLE 6.1: $L^{\infty}_{\Omega\times[0,T]}$ differences between the local continuous solution u^{ℓ} and discrete solution $u^{qnl}_{\delta,\Delta x}$. We fix $\delta = 3\Delta x$, and the kernel is $\gamma_{\delta}(s) = \frac{3}{\delta^3}\chi_{[-\delta,\delta]}(s)$. The termination time $T = 1$ and $\Delta t = 0.2\Delta x$. 77

TABLE 6.2: $L^{\infty}_{\Omega\times[0,T]}$ differences between the local continuous solution u^{ℓ} and discrete solution $u^{qnl}_{\delta,\Delta x}$. We fix $\delta = 3\Delta x$, and the kernel is $\gamma_{\delta}(s) = \frac{3}{\delta^3}\chi_{[-\delta,\delta]}(s)$. The termination time $T = 1$ and $\Delta t = 0.2\Delta x$. 80

FIGURE 2.1: Diffusion flow of particles from higher concentration to lower concentration. 3

FIGURE 2.2: At each point there is equal probability of the next direction choice. Current position is established by averaging the probability of directional choice from the previous step location beginning with the starting point 4

FIGURE 2.3: Domain body of the diffusion problem. 8

FIGURE 2.4: The maximum of the solution is initially, or on the boundaries. 9

FIGURE 2.5: The maximum of the solution is not located at the terminal time. 11

FIGURE 3.1: Horizon δ is the radius of a ball around x where the solutions are averaged creating a vanishing property at singularities. 15

FIGURE 4.1: Partitioning and boundary layer for a one dimensional domain. 29

FIGURE 5.1: Partitioning and boundary layer for a discretized one dimensional domain. 37

FIGURE 5.2: Example finite difference stencil with $\Delta x = \frac{1}{5}$, horizon $\delta = r\Delta x$, and $r = 3$. 40

FIGURE 5.3: Maximum Growth Rate of (5.58), (5.59), (5.60) for the new finite difference method versus that of (5.8) for the original finite difference method. 60

FIGURE 5.4: Plots of solutions to the approximate and actual solutions. The kernel function was chosen as $\gamma_\delta(s) = \frac{3}{\delta^3}\chi_{[-\delta,\delta]}(s)$. The coupling inference is at $x^* = 0$, and the mesh size is $\Delta x = \frac{1}{400}$ with a horizon as $\delta = \frac{3}{400}$, the temporal step size is $\Delta t = 0.45\Delta x$. 62

FIGURE 5.5: Numerical comparison between the new scheme (5.6) and original scheme (5.8) used to approximate (5.72) with external force given by (5.73). The spatial step size is $\Delta x = \frac{1}{200}$ and Δt=$0.25\Delta x$. 64

FIGURE 6.1: Numerical comparison between approximate and actual solution with Neumann Boundary Conditions 77

FIGURE 6.2: Numerical comparison between approximate and actual solution with Robin Boundary Conditions 80

CHAPTER 1: INTRODUCTION

Diffusion is not a new topic, but ample fields of research depend on the basics of the mathematical diffusion process to analyze movement of a variety of different mediums. The most utilized forms of diffusion are local and nonlocal diffusion. Local diffusion is common and well studied, and its uses are broad. It is dependant on cohesive material so communication from one point to the next is without interruption which makes it's solutions easily and quickly numerically developed. Local diffusion research can be found in geology, energy, neuroscience, cancer, and movement of people and ideas. [33] [46] [9] [6]

Nonlocal diffusion is a newer model of solving how something spreads that allows for the space considered to not be cohesive. There can be disconnections in ideas, cracks in material or other versions of singularities. Nonlocal diffusion is interchangeable with local diffusion, but comes with a numerical time expense when used. The benefit of vanishing imperfections still makes the use of nonlocal diffusion popular. Research utilizing nonlocal diffusion can be found in geology, imaging, machine learning, and mechanics to name a few. [7] [21] [36] [5] [12] [39] Due to the reality of time constraints on numerically solving a nonlocal model, there has become a need for coupling nonlocal and local models, and this idea is discussed in greater detail throughout this paper.

First we begin by exploring the continuous model of local diffusion. Specifically, how it is developed, it's useful properties, and uses beyond basic local diffusion problems. Then we follow similarly with a review of the continuous model for nonlocal diffusion. After outlining these two models the next discussion is about the need for a coupling operator to link nonlocal and local diffusion models, and the development of a specific coupling operator that is later discretized and used for numerical approximation experiments and analysis.

Next we propose a finite difference numerical discretization scheme which relates closely to a previously developed scheme, but includes an additional and necessary property of the discretized maximum priniciple. This allows for guaranteed convergence of the approximate solution described by this new proposed finite difference scheme for the given quasi-nonlocal coupling operator. After introducing the development of the finite difference scheme the following three chapters are dedicated to proving the consistency, stability, and convergence of the scheme. In the following chapter we also breifly analyze the Courant-Friedrichs-Lewy (CFL) condition, and provide benchmark examples to further confirm results. We conclude with a comparison of the previous scheme and new scheme approximation results.

The final chapter begins with the derivation of the of the numerical local to nonlocal operator from the continuous local to nonlocal operator of the diffusion problem with Dirichlet boundary conditions. Next we develop the coefficient matrix for the numerical operator with Dirichlet, Neumann, and Robin boundary conditions. Then benchmark examples are provided to analyze the use of the developed numerical local to nonlocal diffusion operator with Neumann and Robin boundary conditions. Finally the results of the numerical local to nonlocal finite difference scheme with the three types of boundary conditions are compared.

CHAPTER 2: LOCAL DIFFUSION

Diffusion is a common problem of study that has produced much information and relevant research in diverse areas. The meaning of diffusion is to spread out, and there are important ideas in several unrelated fields that are concerned with such movement. The net movement of atoms, particles, people, animals, ideas, and prices are a few examples, and these ideas are studied widely in physics, chemistry, biology, sociology, economics, and finance.

2.1 Deriving the Local Diffusion Model

Flick's law is one approach to analyzing diffusion that is centered on an observable phenomena that the rate of diffusion is proportional to the negative gradient of the concentration. This means that particles travel from areas of higher concentration to areas of lower concentration, heat spreads from hotter locations to cooler locations, or people migrate from more populated areas to less populated areas resulting in the uniform distribution of the diffusing substance.

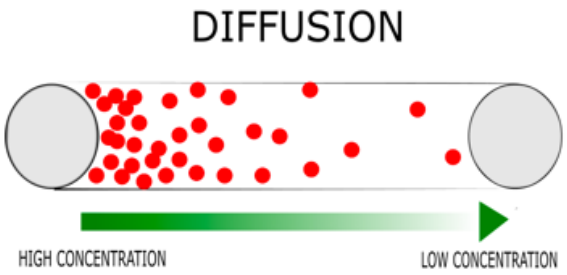

Figure 2.1: Diffusion flow of particles from higher concentration to lower concentration.

Definition 1 (Fick's First Law of Diffusion)**.** *Fick's first law of diffusion is defined by*

$$J = -D\frac{du}{dx}, \tag{2.1}$$

where J is the flux of atoms (the number of particles which pass through a unit area in a unit of time), D is the diffusion coefficient with units area per unit time, and $\frac{du}{dx}$ is the concentration gradient.

The diffusion coefficient D is proportional to the squared velocity of the spreading particles, and the velocity depends on several characteristics of the system. Fick's first law is only applicable for an isotropic and homogeneous medium whose structures and diffusion properties are the same in the neighborhood of any point in all directions, and can only be applied when the flux coming into the system equals the flux going out.

Fick's second law of diffusion is another approach to studying diffusion in an isotropic medium, and is an atomistic view resulting from the random walk of diffusing particles. Fick's second law is more applicable to physical science and other systems where the solution is not equal throughout. This diffusion process can be illustrated as a series of steps that are randomly decided as a particle moves from where it was initially located.

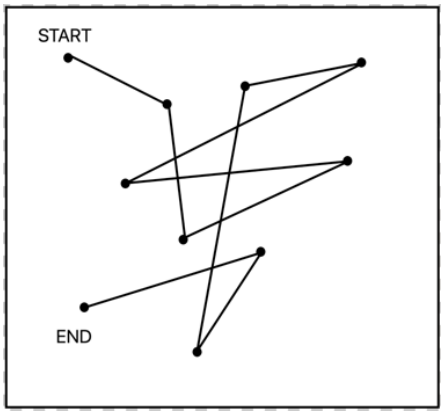

Figure 2.2: At each point there is equal probability of the next direction choice. Current position is established by averaging the probability of directional choice from the previous step location beginning with the starting point

Random walk is a common term used in the development of the theory of diffusion, Brownian motion, and other important applications in finance, economics, and physical sciences. Diffusion is typically spreading of particles or heat that follows Fourier's law of heat conduction. Brownian motion is a macroscopic picture of a particle moving randomly in space without making big jumps, and is used in probability theory to describe random systems defined by microscopic random effects. The difference between a random walk and Brownian motion is that random walk is a discrete space and discrete time model versus a continuous time and continuous space model for Brownian motion.

Definition 2 (Fick's Second Law)**.** *Fick's second law is a partial differential equation defined as*

$$u_t(x,t) = Du_{xx}(x,t), \tag{2.2}$$

where u is concentration, and D is the diffusion coefficient. The solution $u(x,t)$ that satisfies this partial differential equation predicts how diffusion causes the concentration to change with respect to space and time.

A physical interpretation of Fick's second law is that u_{xx} gives the difference between the average value of the function in the neighborhood of a point and its value at that point. If $u(x,t)$ is concentration then u_{xx} is by how much the area around each point varies in density on average from the area at the point. Imagine particles randomly walking from their starting location where $u(x,t)$ is concentration at location x and time t, and $r(x,t)$ is the rate at which particles cross the point x at time t. Particles cannot be created nor destroyed therefore the rate the particles leave $[a,b]$ in terms of $r(x,t)$ is

$$r(b,t) - r(a,t) = \int_a^b \frac{\partial}{\partial x} r(x,t)dx. \tag{2.3}$$

The density of a point (particle) in $[a,b]$ is equal to the integral of the concentration, so the

rate the particles leave $[a, b]$ can also be written

$$-\frac{\partial}{\partial t}\int_a^b u(x,t)dx = -\int_a^b \frac{\partial}{\partial t}u(x,t)dx. \tag{2.4}$$

Combining the equal rates of the particles leaving $[a, b]$ gives

$$-\int_a^b \frac{\partial}{\partial t}u(x,t)dx = \int_a^b \frac{\partial}{\partial x}r(x,t)dx \tag{2.5}$$

resulting in the *conservation law.*

Definition 3 (Law of Conservation)**.** *For concentration $u(x,t)$ and the rate at which particles cross the point x at time t defined as $r(x,t)$ the conservation law is*

$$\frac{\partial u}{\partial t} = -\frac{\partial r}{\partial x}. \tag{2.6}$$

Particle movement is random, but it is known that particles move from more concentrated areas to less concentrated areas. Particles are also affected by the spatial rate of change of the density u_x. Any relationship that describes the rate (r) at which particles leave the interval $[a, b]$ in terms of space (x), concentration (u), and spatial derivative (u_x) is called a constituitive law. This leads to the most common *constituitive law* supported by experimental evidence.

Definition 4 (Constituitive Law)**.** *For concentration $u(x,t)$ and the rate at which particles cross the point x at time t defined as $r(x,t)$ the constituitive law is*

$$r(x,t) = -D\frac{\partial u}{\partial x}, \tag{2.7}$$

where $D > 0$, and $-D$ represents that the particles move to less dense areas.

Combining the *conservation* and the *constituitive* laws gives

$$\frac{\partial u}{\partial t} = -\frac{\partial r}{\partial x} = -\frac{(-D\frac{\partial u}{\partial x})}{\partial x} = D\frac{\partial^2 u}{\partial x^2}, \tag{2.8}$$

and the combination of these two laws lead to the basic diffusion equation

$$u_t(x,t) = Du_{xx}(x,t). \tag{2.9}$$

More formally,

Definition 5. *Total Heat is defined*

$$H(t) = \int_\Omega c\rho u(x,t)dx \tag{2.10}$$

where c is the specific heat of the material, and ρ is it's density.

Theorem 1. *The heat equation is derived from the rate of heat in the system.*

Proof. To find the rate of heat we take the derivative of the total heat.

$$\frac{dH}{dt} = \int_\Omega c\rho u_t(x,t)dx. \tag{2.11}$$

Fourier's law of thermal conduction states the negative gradient of temperature and rate of heat is proportional to the gradient of the heat flow. Combined with the property that heat leaves the domain through the boundary we can also write the rate of heat as

$$\frac{dH}{dt} = \int_{\partial\Omega} \kappa\nabla u \cdot \hat{n}ds \tag{2.12}$$

where constant $\kappa > 0$ when heat flows from hot to cold regions. Now we compare the

equivalencies of the two rates and utilize the divergence theorem to find the following results

$$\begin{aligned}\int_\Omega c\rho u_t dx &= \int_{\partial\Omega} \kappa\nabla u \cdot \hat{n} ds \\ &= \int_\Omega \nabla \cdot (\kappa\nabla u) dx \\ &= \int_\Omega \kappa\Delta u dx. \end{aligned} \tag{2.13}$$

Let $D = \frac{\kappa}{c\rho}$ then

$$u_t = D\Delta u, \tag{2.14}$$

and since the total heat rate is the sum of the rate of heat leaving the system and any rate of heat added by a heat source the heat equation can be defined

$$u_t = D\Delta u + f \tag{2.15}$$

where f is an added heat source rate. □

2.2 Properties of Local Diffusion

Now we will discuss properties of the general solution of the diffusion problem. Consider a space/time rectangular region where $0 \leq x \leq L$ and $0 \leq t \leq T$, and let $R = [0, L] \times [0, T]$.

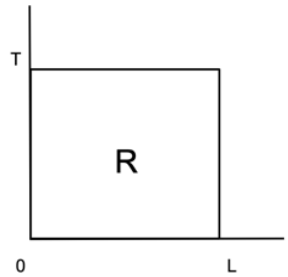

Figure 2.3: Domain body of the diffusion problem.

Physically the initial temperature or density, as well as the temperature or density on the boundaries will dissipate or diffuse through conduction. Thermally vibrating molecules pass their kinetic energy to adjacent molecules, and in gases and liquids, conduction is due to the collisions and diffusion of molecules during their random motion. This leads us to the *Maximum Principle Property.*

Theorem 2. ***Maximum Principle for the Local Diffusion Equation*** *If $u(x,t)$ satisfies the diffusion equation in R then the maximum value of $u(x,t)$ over R is either initially, or on the boundaries.*

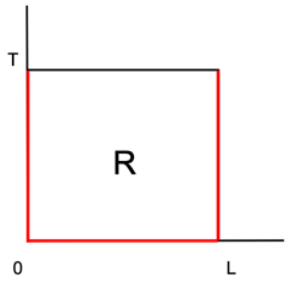

Figure 2.4: The maximum of the solution is initially, or on the boundaries.

Proof. Assume for contradiction there exists an internal point (x_0, t_0) in $R\backslash\Gamma$ such that the maximum of $u(x,t)$ is at $u(x_0,t_0)$. Then since $u(x_0,t_0)$ is the maximum by the first derivative test $u_t(x_0,t_0) = u_x(x_0,t_0) = 0$, and by the second derivative test $u_{xx}(x_0,t_0) \leq 0$.

Case I: $u_{xx}(x_0,t_0) < 0$

Then inserting $u(x_0,t_0)$ in the diffusion equation gives

$$u_t(x_0,t_0) - Du_{xx}(x_0,t_0) = 0 - Du_{xx}(x_0,t_0) > 0, \tag{2.16}$$

but this contradicts the diffusion equation $u_t - Du_{xx} = 0$. Therefore the maximum value cannot be an internal point.

Case II: $u_{xx}(x_0,t_0) = 0$

Let $\epsilon > 0$ and define

$$v(x,t) = u(x,t) + \epsilon x^2. \tag{2.17}$$

Now let the boundaries and initial time be $\Gamma = \{t = 0 \cup x = 0 \cup x = L\}$, and

$$\begin{aligned} M &= \max\{u(x,t) : (x,t) \in \Gamma\} \\ m &= \max\{u(x,t) : (x,t) \in R\}. \end{aligned} \tag{2.18}$$

Since $\Gamma \subset R$ we know $M \leq m$, and for any point in Γ we have $v(x,t) \leq M + \epsilon L^2$. Next for any point in R from the definition of $v(x,t)$ we can write

$$u(x,t) \leq v(x,t) - \epsilon x^2 \leq M + \epsilon(L^2 - x^2). \tag{2.19}$$

Since $(L^2 - x^2)$ is bounded in R by taking ϵ small enough then

$$u(x,t) \leq M, \qquad \text{for all } \ (x,t) \in R. \tag{2.20}$$

Observe that inserting $v(x,t)$ into the diffusion equation leads to

$$v_t - Dv_{xx} = u_t - D(u_{xx} + 2\epsilon) = (u_t - Du_{xx}) - 2D\epsilon < 0 \tag{2.21}$$

since $D > 0$, $\epsilon < 0$, and $u_t - Du_{xx} = 0$. Therefore,

$$v_t - Dv_{xx} < 0, \qquad \text{for all } \ (x,t) \in R. \tag{2.22}$$

Similarly as before, we assume that the maximum of $v(x,t)$ happens at an interior point (x_0, t_0) in $R \backslash \Gamma$. Then observe that the properties of the maximum, $v_t(x_0,t_0) = 0$ and $v_{xx}(x_0,t_0) \leq 0$, yield

$$v_t(x_0, t_0) - Dv_{xx}(x_0, t_0) = -Dv_{xx}(x_0, t_0) \geq 0. \tag{2.23}$$

This contradicts $v_t - Dv_{xx} < 0$ which means the maximum of $v(x,t)$ is not at an interior point.

Finally, assume $v(x,t)$ has a maximum at $t = T$.

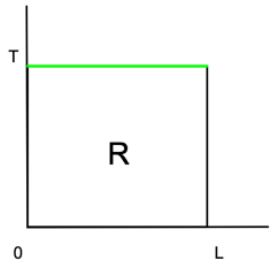

Figure 2.5: The maximum of the solution is not located at the terminal time.

Then $v_x(x,T) = 0$, $v_{xx}(x,T) \leq 0$, $v_t(x,T)$ is unknown. To construct $v_t(x,T)$, we use the limit definition of a derivative.

$$\lim_{h \to 0^+} \frac{v(x,T) - v(x,T-h)}{h} \geq 0, \tag{2.24}$$

since $v(x,T)$ is the assumed maximum, and the difference between a maximum and anything else is positive or zero. This again contradicts $v_t - Dv_{xx} < 0$ which means the maximum of $v(x,t)$ is not at t=T.

We have eliminated any possibility that the maximum for $v(x,t)$ is located anywhere in R other than in Γ which consists of the initial time and boundaries. We have also proved that this maximum is bounded, so by the definition $v(x,t) = u(x,t) + \epsilon x^2$ and the ability to take ϵ small enough we achieve that the maximum of $u(x,t)$ is bounded and in Γ. Precisely, $M = m$. □

Another important thing to consider when working with the diffusion equation is whether or not the system of the partial differential equation is well-posed. That is the solution exists, is unique, and is stable.

Now that we proved the solution to the classical diffusion equation exists by constructing a general solution based on specified initial and boundary conditions, we will confirm the solution's uniqueness and stability. Uniqueness can be proven in two ways. One way is to assume there are two different solutions that are not equal and then show they are, or similarly by an energy method.

Theorem 3. *The solution $u(x,t)$ is unique for (x,t) in R.*

Proof. METHOD 1: Assume u and v both solve the diffusion equation for (x,t) in R such that $w = u - v$ and satisfies the diffusion equation. Then by the maximum principle w achieves a maximum in Γ, so $w = 0$ on the boundaries or initially. To finish the analysis of the solution's uniqueness, we need to add an initial condition, and boundary conditions. Assume the initial condition is $u(x,0) = 0$, and the boundary conditions are $u(0,t) = u(L,t) = 0$. Then we can conclude that $0 \leq w \leq 0$, $w(x,t) = 0$, and $u = v$. Therefore the solution is unique.

METHOD 2: Again Assume u and v both solve the diffusion equation for (x,t) in R such that $w = u - v$ and satisfies the diffusion equation. Also consider the same initial and boundary conditions. Define the energy

$$E = \frac{1}{2}\int_0^L (w(x,t))^2 dx. \tag{2.25}$$

Then E is nonnegative, and differentiating with respect to time results in

$$\frac{d}{dt}E = \int_0^L w w_t dx = -D\int_0^L w w_{xx} dx. \tag{2.26}$$

Next, combining integration by parts and the boundary conditions give

$$\frac{d}{dt}E = -D\int_0^L w_x^2 dx \leq 0 \tag{2.27}$$

This demonstrates that that E is decreasing, so since E is always positive, decreasing, and has an initial condition of $w(x,0) = 0$ then

$$0 \leq E = 0. \tag{2.28}$$

This leads back to $w = 0$, and $u = v$. Therefore the solution is unique. □

The last condition of a well-posed partial differential equation is stability. Stability is when, for any initial condition, the solution of the diffusion equation is bounded.

Theorem 4. *The solution to the diffusion equation is stable.*

Proof. Consider again solutions u, v, and w that satisfy the diffusion equation such that $w = u - v$. Also assume we have the initial and boundary conditions

$$\begin{aligned} u(x,0) &= f_1(x) \\ u(0,t) &= g_1(t) \\ u(L,t) &= h_1(t), \end{aligned} \tag{2.29}$$

and

$$\begin{aligned} v(x,0) &= f_2(x) \\ v(0,t) &= g_2(t) \\ v(L,t) &= h_2(t). \end{aligned} \tag{2.30}$$

This implies

$$\begin{aligned} w(x,0) &= f_1(x) - f_2(x) \\ w(0,t) &= g_1(t) - g_2(t) \\ w(L,t) &= h_1(t) - h_2(t). \end{aligned} \tag{2.31}$$

Next the maximum/minimum principle leads to

$$-\max\{|w(x,t)| : (x,t) \in \Gamma\} \leq \max\{w(x,t) : (x,t) \in R\} \leq \max\{|w(x,t)| : (x,t) \in \Gamma\} \tag{2.32}$$

Therefore,

$$\begin{aligned} \max\{|u-v| : (x,t) \in R\} &= \max\{|w| : (x,t) \in R\} \leq \max\{|w(x,t)| : (x,t) \in \Gamma\} \\ &= \max\{|f_1(x) - f_2(x)|, |g_1(t) - g_2(t)|, |h_1(t) - h_2(t)| : (x,t) \in R\}. \end{aligned} \tag{2.33}$$

This implies the closeness of the conditions bound the solutions which provides uniform stability.

□

2.3 Local Diffusion Conclusion

In this chapter we introduced the local diffusion problem. We looked at how it was developed through Fick's, conservation, and constituitive laws. Then we explored and proved the properties that are a result of the maximum/minimum principle and necessary for a well posed partial differntial equation including existence, uniqueness, and stability. The next chapter will focus on the nonlocal diffusion problem.

CHAPTER 3: NONLOCAL DIFFUSION

The study of the nonlocal diffusion problem stems largely from the nonlocal continuum theory called peridynamics. This is the study of governing equations that are usable at discontinuities. In these governing equations, the spatial derivatives which are unknown at discontinuities are replaced with integrals that are known at the discontinuities. This is the main difference between classical local partial differential governing equations and nonlocal models. The integral operators that are used for nonlocal modeling create accurate results by providing a space for singularities and discontinuous points in a countable way so that they can be omitted or jumped over by a vanishing property.

The vanishing property is the result of the the nonlocal model including a kernel function designed by a specific choice of horizon δ. The horizon is the effective range of the nonlocal interactions, and as $\delta \to 0$, the nonlocal model reduces to the local model. The radius is determined by the values that create the null space in the domain and solutions are averaged within the ball by vanishing at singularities.The following image of how the horizon is used to associate a point x with it's neighbors within a neighborhood of radius δ.

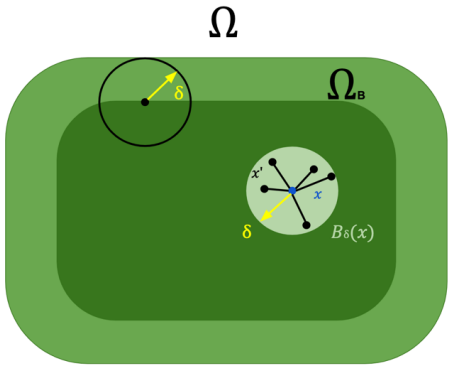

Figure 3.1: Horizon δ is the radius of a ball around x where the solutions are averaged creating a vanishing property at singularities.

In this chapter topics discussed are influenced by the following references throughout [2], [25], [1], [37], [42], [8], [17], [40], [38], [16], [12].

3.1 Deriving the Nonlocal Diffusion Model

Nonlocal diffusion can be viewed as the evolution of a Guassian distribution where the solution evolves by trying to increase in time at points where the mean value is larger than the value at the point and to decrease when the mean value is smaller [37]. A common choice to model nonlocal diffusion problem is

$$u_t(x,t) = \int_{R^N} J(x-y)(u(y,t) - u(x,t))dy. \tag{3.1}$$

Here $J : R^N \to R$ is nonnegative, smooth, and $\int_{R^N} J = 1$. Also $J(x-y)$ is the probability distribution of jumping from y to x. The basic local diffusion model only needs the value of u at x when u_{xx} is at point x, but the nonlocal model needs the value of u at points $y \neq x$ at the point x when u_{xx} is at point x.

Consider the nonlocal Laplacian $(-\Delta)^{\frac{\alpha}{2}}$ such that $0 < \alpha < 2$. This is a nonlocal operator, and unlike its local counterpart it is not possible to compute its value only using u in a arbitrarily small neighborhood of x. Some examples of nonlocal operators are the following.

Definition 6. *Nonlocal Operators*

Fourier transform

$$\mathcal{F}\{u(x)\} = \int_{\infty}^{\infty} u(x)e^{-i(2\pi\xi)x}dx. \tag{3.2}$$

Laplace transform

$$\mathcal{L}\{u(x)\} = \int_{0}^{\infty} u(x)e^{-st}dx. \tag{3.3}$$

Singular integral transform

$$\mathcal{T}\{u(x)\} = \int K(x,y)u(y)dy \tag{3.4}$$

where $K(x,y)$ is called the kernel function and is singular along the diagonal $x = y$.

The singular integral transform is our further focus, and this transform allows only the need of support for f almost everywhere excluding where $K(x,y)$ has finitely many singularities. The singular integral operator is developed through convolutions of distributions, or commutes with translations. An example of a singular integral operator is the fractional Laplacian.

Definition 7. *Fractional Laplacian Operator*

$$(-\Delta)^{\frac{\alpha}{2}}u(x) = \frac{C(n,\frac{\alpha}{2})}{2}\int_{R^n}\frac{2u(x)-u(x+y)-u(x-y)}{|y|^{n+\alpha}}dy \tag{3.5}$$

$C(n,\frac{\alpha}{2})$ is a constant.

This fractional Laplacian operator can model diffusion, and it can be shown this operator performs as we expect.

Theorem 5. *If $(-\Delta)^{\frac{\alpha}{2}}u(x)$ is the fraction Laplacian operator then*

$$u_t(x,t) = (-\Delta)^{\frac{\alpha}{2}}u(x). \tag{3.6}$$

Proof. First consider the probability distribution

$$P(N) = C\sum_{n\in N}\frac{1}{|n|^{1+\alpha}} = 1. \tag{3.7}$$

Then the constant is

$$C = \left(\sum_{n\in N}\frac{1}{|n|^{1+\alpha}}\right)^{-1}. \tag{3.8}$$

Let $u(x,t)$ represent the probability of finding the particle at the point x and time t, and B be a neighborhood around x. Let h be the step size of the spatial discretization. The direction the particle chooses randomly is represented by $v \in \partial B$, and moves by a discrete time step h. This leads to the probability of finding a particle at x and time $t+h$ as the sum of the probabilities of finding the particle elsewhere, or

$$u(x,t+h) = \frac{C}{|\partial B|} \sum_{n \in N} \int_{\partial B} \frac{u(x+nhv,t)}{|n|^{1+\alpha}} dv \tag{3.9}$$

where $\frac{C}{|\partial B|}$ is a constant that normalizes the probability. Then taking the limit and imposing Reimann sum gives

$$\begin{aligned} u_t(x,t) &\simeq \lim_{h \to 0} \frac{u(x,t+h) - u(x,t)}{h} \\ &= \frac{C}{|\partial B|} \sum_{n \in N} \int_{\partial B} \frac{u(x+nhv,t)}{|nh|^{1+\alpha}} dv - \frac{C}{|\partial B|} \sum_{n \in N} \int_{\partial B} \frac{u(x,t)}{|nh|^{1+\alpha}} dv \\ &= \frac{C}{|\partial B|} \sum_{n \in N} \int_{\partial B} \frac{u(x+nhv,t) - u(x,t)}{|nh|^{1+\alpha}} dv. \end{aligned} \tag{3.10}$$

$u(x,t)$ is symmetric since it is a normalized probability, so

$$\begin{aligned} &\frac{C}{|\partial B|} \sum_{n \in N} \int_{\partial B} \frac{u(x+nhv,t) - u(x,t)}{|nh|^{1+\alpha}} dv \\ &= \frac{C}{2|\partial B|} \sum_{n \in N} \int_{\partial B} \frac{u(x+nhv,t) + u(x-nhv,t) - 2u(x,t)}{|nh|^{1+\alpha}} dv \end{aligned} \tag{3.11}$$

Let $s = nh$; now we have

$$\begin{aligned} u_t(x,t) &\simeq \frac{C}{2|\partial B|} \sum_{n \in N} \int_{\partial B} \frac{u(x+nhv,t) + u(x-nhv,t) - 2u(x,t)}{|nh|^{1+\alpha}} dv \\ &\simeq \frac{C}{2|\partial B|} \int_0^\infty \int_{\partial B} \frac{u(x+sv,t) + u(x-sv,t) - 2u(x,t)}{|s|^{1+\alpha}} ds \\ &= \frac{C}{2|\partial B|} \int_{R^n} \frac{u(x+y,t) + u(x-y,t) - 2u(x,t)}{|y|^{n+\alpha}} dy \\ &= (-\Delta)^{\frac{\alpha}{2}} u(x,t). \end{aligned} \tag{3.12}$$

□

This demonstrates a fractional Laplacian with a probabilistic process, and with small enough step sizes this equation will approach the diffusion equation.

Next we will review the development of a more compact form of the previous diffusion equation.

Theorem 6. *The fraction Laplacian operator* $(-\Delta)^{\frac{\alpha}{2}} u(x,t)$ *has the following equivalency*

$$(-\Delta)^{\frac{\alpha}{2}} u(x,t) = (-\Delta)^{\alpha/2} u(x) = C(n, \frac{\alpha}{2}) \int_{R^N} \frac{u(x) - u(y)}{|x-y|^{n+\alpha}} dy. \tag{3.13}$$

Proof. Recall the original form of the fraction Laplacian then rearranging and utilizing change of variables and the symmetry of $u(x,t)$ leads to

$$
\begin{aligned}
(-\Delta)^{\frac{\alpha}{2}}u(x,t) &= \frac{C(n,\frac{\alpha}{2})}{2}\int_{R^n\setminus B_\delta(x)}\frac{2u(x)-u(x+y)-u(x-y)}{|y|^{n+\alpha}}dy \\
&= \frac{C(n,\frac{\alpha}{2})}{2}\lim_{\delta\to 0}\int_{R^n}\frac{2u(x)-u(x+y)-u(x-y)}{|y|^{n+\alpha}}dy \\
&= \frac{C(n,\frac{\alpha}{2})}{2}\lim_{\delta\to 0}\left(\int_{R^n\setminus B_\delta(x)}\frac{u(x)-u(x+y)}{|y|^{n+\alpha}}+\int_{R^n\setminus B_\delta(x)}\frac{u(x)-u(x-y)}{|y|^{n+\alpha}}dy\right) \\
&= \frac{C(n,\frac{\alpha}{2})}{2}\lim_{\delta\to 0}\left(\int_{R^n\setminus B_\delta(x)}\frac{u(x)-u(\eta)}{|y|^{n+\alpha}}+\int_{R^n\setminus B_\delta(x)}\frac{u(x)-u(\xi)}{|y|^{n+\alpha}}dy\right) \\
&= C(n,\frac{\alpha}{2})\lim_{\delta\to 0}\int_{R^n\setminus B_\delta(x)}\frac{u(x)-u(\eta)}{|x-\eta|^{n+\alpha}}dy. \qquad (3.14)
\end{aligned}
$$

Therefore, $(-\Delta)^{\alpha/2}u(x)$ can be written in a more usable way.

$$
(-\Delta)^{\alpha/2}u(x) = C(n,\frac{\alpha}{2})\int_{R^N}\frac{u(x)-u(y)}{|x-y|^{n+\alpha}}dy \qquad (3.15)
$$

□

Similarly to the classical Laplacian this equation uses the elastic property, or ability to return to equilibrium after a force is applied, of the harmonic function whose values at each point are the average in a ball. The integral component of the fractional Laplacian is defined as the principle value

Definition 8. *Principle Value Equation*

A method for assigning values for undefined values of improper integrals.

$$
PV = \int_{R^N}\frac{u(x)-u(y)}{|x-y|^{n+\alpha}}dy \qquad (3.16)
$$

In general, when y is in the neighborhood of x there is a singularity that is not integrable, but the principle value averages out in a neighborhood of x by symmetry.

Recall the common choice for a nonlocal diffusion model discussed at the beginning of this chapter, $u_t(x,t) = \int_{R^N} J(x-y)(u(y,t)-u(x,t))dy$. Compared with the compact fractional

Laplacian, they both have a component that can jump over discontinuities by vanishing at their locations. This component that vanishes at irregularities is called the kernel.

Definition 9. *Kernel*

The kernel is commonly discussed as $\gamma(x, y)$. *Let the* Ω_B *be the domain containing the boundary values,* Ω_I *be the interior domain, and* $\Omega = \Omega_B \cup \Omega_I$. *For* $\delta > 0$, *and all* x *in* Ω

$$\gamma(x, y) = 0 \text{ when } y \text{ is in } \Omega \backslash B_\delta(x). \tag{3.17}$$

Therefore interactions are nonlocal but only in a small neighborhood around x. Other nice properties of the kernel include that it is continuous, symmetric or even, non negative, and its integral on Ω equals 1 almost everywhere.

A nonlocal boundary value problem is written by utilizing the nonlocal operator to account for nonlocal effects.

$$\begin{cases} u_t(x,t) = \mathcal{L}u(x,t) \\ u(x,0) = f(x) \\ u(0,t) = u(L,t) = 0 \end{cases}$$

where the nonlocal diffusion operator is defined.

Definition 10. *Nonlocal Diffusion Operator*

$$\mathcal{L}u(x,t) = \int_{-\delta}^{\delta} \gamma(s)(u(x+s,t) - u(x,t))ds. \tag{3.18}$$

Now we will discuss the properties of the nonlocal diffusion problems.

3.2 Properties of Nonlocal Diffusion

This section begins with a review of the contraction mapping theorem, or the Banach fixed point theorem. This is the tool used to guarantee the existence and uniqueness of fixed

points in certain spaces. The theorem also provides a construction to find the fixed points. To show that the nonlocal homogeneous Dirichlet boundary value problem is well-posed first we prove the existence and uniqueness of the solution then the convergence, or stability of the solution.

Theorem 7. ***Banach Fixed Point Theorem.***

Let (Ω, d) be a non-empty complete metric space with contraction mapping $T : \Omega \to \Omega$. Then mapping T takes a fixed point x^* in Ω such that $T(x^*) = x^*$. This allows x^* to be found by selecting an arbitrary x_0 in Ω and defining a sequence $\{x_n\}_n$ by $x_n = T(x_{n-1})$ for $n \geq 1$. Then the limit of this section converges to x^*. (i.e. $\lim_{n\to\infty} x_n = x^*$).

Proof. Since T is a contraction mapping, for constant c such that $0 \leq c < 1$, and sequence $\{x_n\}_n$ such that $x_n = T(x_{n-1})$

$$||x_2 - x_1|| = ||T(x_1) - T(x_0)|| = ||T(T(x_0)) - T(x_0)|| \leq c||T(x_0) - x_0|| = c||x_1 - x_0||. \tag{3.19}$$

This leads to the generalization

$$||x_n - x_{n-1}|| = ||T(x_{n-1}) - T(x_{n-2})|| \leq c||x_{n-1} - x_{n-2}||. \tag{3.20}$$

Then by induction

$$||x_n - x_{n-1}|| \leq c^{n-1}||T(x_0) - x_0||, \tag{3.21}$$

so for m such that $m > n-1$ the triangle inequality gives

$$\begin{aligned} ||x_m - x_{n-1}|| &\leq ||x_m - x_{m-1}|| + ||x_{m-1} - x_{m-2}|| + \cdots + ||x_n - x_{n-1}|| \\ &\leq [c^{m-1} + c^{m-2} + \cdots + c^{n-1}] \cdot ||T(x_0) - x_0|| \\ &= c^{n-1}[1 + c + \cdots + c^{(m-1)-(n-1)}] \cdot ||T(x_0) - x_0|| \\ &= c^{n-1} \cdot \frac{1 - c^{m-n-1}}{1-c} \cdot ||T(x_0) - x_0||. \end{aligned} \tag{3.22}$$

Also since $0 \leq c < 1$ if $m > n-1$

$$||x_m - x_{n-1}|| \leq \frac{c^{n-1}}{1-c} \cdot ||T(x_0) - x_0||, \tag{3.23}$$

and

$$\sum_{n=1}^{k} c^{n-1} = \frac{1 - c^{k+1}}{1-c}. \tag{3.24}$$

The $\lim_{n\to\infty} c^{n-1} = 0$, so

$$||x_m - x_{n-1}|| \to 0. \tag{3.25}$$

This means the sequence $\{x_{n-1}\}$ is a Cauchy sequence in a complete metric space which gives that there is a point x in Ω such that $x_n \to x$. Then since T is Lipschitz continuous

$$T(x) = \lim_{n\to\infty} T(x_{n-1}) = \lim_{n\to\infty} x_n = x, \tag{3.26}$$

or T has at least one fixed point. Next assume s and t are fixed points in Ω. Then since $0 \leq c < 1$

$$0 \leq ||s - t|| = ||T(s) - T(t)|| \leq c||s - t|| \leq ||s - t|| \tag{3.27}$$

giving $||s-t|| = 0$, and $s = t$. Therefore there is only one fixed point. □

Consider the nonlocal Dirichlet boundary value problem defined as

$$\begin{cases} u_t(x,t) = \int_{R^N} J(x-y)(u(y,t)-u(x,t))dy \\ u(x,0) = u_0(x) \\ u(0,t) = u(L,t) = 0 \end{cases}$$

where $x \in \Omega = [0, L]$, and $t > 0$. Then the solution is the function

$$u(x,t) = u_0(x) + \int_0^t \int_{R^N} J(x-y)(u(y,s)-u(x,s))dyds \tag{3.28}$$

where $u \in C([0,\infty); L^1(R^N))$.

Theorem 8. *The solution* $u(x,t) = u_0(x) + \int_0^t \int_{R^N} J(x-y)(u(y,s)-u(x,s))dyds$ *of the nonlocal diffusion Dirichlet boundary value problem exists and is unique for every* $u_0(x) \in L^1(\Omega)$.

Proof. Fix $t_0 > 0$ also define a Banach space $X_{t_0} = \{w \in C[0,t_0]; L^1(\Omega)\}$ with norm

$$||w|| = \max_{0 \le t \le t_0} ||w(\cdot,t)||_{L^1(\Omega)} \tag{3.29}$$

Then the solution can be found as a fixed point of the operator $T : X_{t_0} \to X_{t_0}$ by

$$T_{w_0}(w)(x,t) = w_0(x) + \int_0^t \int_{R^N} J(x-y)(w(y,s)-w(x,s))dyds \tag{3.30}$$

where $w(x,t)$ follows the same boundary conditions of $u(x,t)$. Next for $w_0, z_0 \in L^1(\Omega)$,

$$\begin{aligned}
&||T_{w_0}(w) - T_{z_0}(z)|| = \int_\Omega |T_{w_0}(w)(x,t) - T_{z_0}(z)(x,t)|dx \\
&\leq \int_\Omega |w_0 - z_0|(x)dx \\
&+ \int_\Omega \Big| \int_0^t \int_{R^N} J(x-y)\Big[(w(y,s) - z(y,s)) - (w(x,s) - z(x,s))\Big]dyds\Big|dx, \qquad (3.31)
\end{aligned}$$

and since $w - z$ is zero outside of Ω

$$||T_{w_0}(w) - T_{z_0}(z)|| \leq ||w_0 - z_0||_{L_1(\Omega)} + Ct_0||w - z|| \qquad (3.32)$$

for some constant C dependent on $J(x-y)$.

Now take $z_0 = 0$, and $z = 0$, and for $\in L^1(\Omega)$ consider $T_{u_0}(w)(x,t)$ for $u_0(x) \in L_1(\Omega)$. Then

$$||T_{u_0}(w)|| = ||T_{u_0}(w) - T_0(0)|| \leq ||u_0 - 0||_{L^1(\Omega)} + Ct_0||w - 0|| = ||u_0||_{L^1(\Omega)} + Ct_0||w|| \qquad (3.33)$$

Therefore, $T_{u_0}(w) \in C([0,t_0]; L^1(\infty))$ for any $w \in X_{t_0}$. Next choose t_0 such that $Ct_0 < 1$ while taking $z_0 = w_0 = u_0$. Then

$$||T_{u_0}(w) - Tu_0(z)|| \leq Ct_0||w - z||. \qquad (3.34)$$

Giving us that T_{u_0} is a contraction mapping of X_{t_0}. Finally we can conclude from Banach's Fixed Point Theorem that $u(x,t)$ exists and is unique in $[0,t_0]$. To extend to $[0,\infty)$ one can take initial data $u(x,t_0) \in L^1(\Omega)$, obtain the solution up to $[0,2t_0]$, and iterate to obtain a solution on $[0,\infty)$.

□

To show the solution to this nonlocal boundary value problem is stable we analyze the

convergence of the solution. For the diffusion equation exponential decay is given by the first eigenvalue, and the asymptotic behaviour of the solution is described by the unique associated eigenfunction.

Theorem 9. *The solution $u(x,t)$ to the nonlocal homogeneous Dirichlet boundary value problem is stable for $u_0 \in L^2(\Omega)$.*

Proof. Let the first eigenvalue of the nonlocal boundary value problem be

$$\lambda_1 = \inf_{u \in L^2(\Omega)} \frac{\frac{1}{2}\int_{R^N}\int_{R^N} J(x-y)(\bar{u}(x)-\bar{u}(y))^2 dxdy}{\int_\Omega (u(x))^2 dx} \tag{3.35}$$

such that

$$\bar{u}(x) = \begin{cases} u(x) \ \text{ if } \ x \in \Omega \\ 0 \ \text{ else.} \end{cases} \tag{3.36}$$

By differentiating and reorganizing, this gives λ_1 as the solution of

$$(1-\lambda_1)u(x) = \int_{R^N} J(x-y)\bar{u}(y)dy \tag{3.37}$$

for $x \in \Omega$. Here $u(x)$ can be considered the eigenfunction corresponding to the first eigenvalue λ_1. Also, if $u(x)$ is non negative it is always positive in Ω, and λ_1 is a positive simple eigenvalue such that $\lambda_1 < 1$. Then because of the symmetry of J

$$\begin{aligned} \frac{\partial}{\partial t}\left(\frac{1}{2}\int_\Omega u^2(x,t)dx\right) &= \int_{R^N}\int_{R^N} J(x-y)(u(y,t)-u(x,t))u(x,t)dydx \\ &= -\frac{1}{2}\int_{R^N}\int_{R^N} J(x-y)(u(y,t)-u(x,t))^2 dydx. \end{aligned} \tag{3.38}$$

Therefore, by the definition of λ_1

$$\frac{\partial}{\partial t}\int_\Omega u^2(x,t)dx \leq -2\lambda_1 \int_\Omega u^2(x,t)dx. \tag{3.39}$$

This gives for $u_0 \in L^2(\Omega)$

$$\int_\Omega u^2(x,t)dx \leq e^{-2\lambda_1 t} \int_\Omega u_0^2(x)dx, \tag{3.40}$$

or

$$||u(\cdot,t)||_{L^\infty(\Omega)} \leq Ce^{-\lambda_1 t} \to 0 \tag{3.41}$$

since $\lambda_1 < 1$. This provides the convergence conclusion needed to show the solution to the nonlocal homogeneous diffusion problem us stable.

□

The completion of the proofs in this section provide all of the properties to conclude that the nonlocal diffusion boundary value problem is well-posed and satisfies the maximum principle.

3.3 Nonlocal Diffusion Conclusion

In this chapter we introduced the nonlocal diffusion problem. We looked at how it was developed through Guassian distribution and its usefulness when dealing with discontinuities. A general solution was defined, and we proved the well posedness of the nonlocal diffusion problem by the solutions existence, uniqueness, and stability. We also proved the properties that are a result of the maximum/minimum principle. The next chapter will focus on coupling nonlocal and local diffusion problems.

CHAPTER 4: COUPLING NONLOCAL AND LOCAL DIFFUSION

Nonlocal modeling can be used for solving even classic local diffusion problems, but although very accurate the computation time can become an obstacle with more refinement. Luckily, most singularities and discontinuities can be isolated so the domain can be partitioned in a way to utilize nonlocal models only where needed and local partial differential equations on the rest of the domain. Local to nonlocal models have emerged as a way to resolve the issue of computational costs of using nonlocal models alone, and also to resolve the issues that come with the complexities of nonlocal boundary conditions. This chapter is based on information that can be found in the following texts [28], [17], [22], [11], [27], [29], [30], [14].

There are several categories of approaches to the coupling of local and nonlocal diffusion models which include generalized domain decomposition, atomistic to continuum coupling, energy based, and force based methods. The focus of the research presented in this dissertation falls into the atomistic to continuum methodology. These types of couplings are designed by linking local and nonlocal diffusion models with a transition region where the domains of each section do not overlap. To develop this operator that partitions the domain between local and nonlocal affects, we look to conservation laws.

Figure 4.1 shows the following decomposition of the domain into nonlocal, transitional, local, and boundary regions respectively. $\Omega = [-1-\delta, 1]$, $\Omega_{NL} = (-1, 0)$, $\Omega_T = [0, \delta)$, $\Omega_L = [\delta, 1)$, and $\Omega_B = [-1-\delta, -1] \cup \{1\}$ where $\Omega = \Omega_{NL} \cup \Omega_L \cup \Omega_T \cup \Omega_B$. δ is called the horizon and is scaled to create an effective interaction range that will capture the singularities.

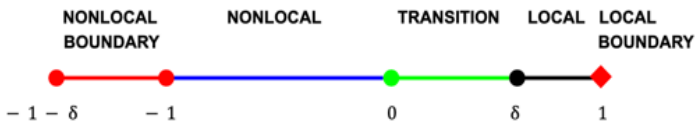

Figure 4.1: Partitioning and boundary layer for a one dimensional domain.

One-dimensional local and nonlocal energy is defined as

Definition 11. *Local and Nonlocal Energies*

One-dimensional Local Energy

$$E_L = \frac{1}{2}\int_{\Omega_L} \omega_\delta(x)|u'(x)|^2 dx, \tag{4.1}$$

(This local energy description is based on a weight function choice of $\omega_\delta(x) = \int_0^1 dt \int\limits_{|s|<\frac{x}{t}} |s|^2\gamma(|s|)ds.$*)*

One-dimensional Nonlocal Energy

$$E_{NL} = \frac{1}{2}\int\limits_{\Omega_{NL}}\int\limits_{\Omega_{NL}} \gamma_\delta(y-x)(u(y)-u(x))^2 dxdy \tag{4.2}$$

where $\gamma_\delta(y-x)$ *is a symmetric kernel, and the relationship between* y *and* x *is called a bond(or the "bond"* $y-x$*).*

To combine the two energies the nonlocal energy is redefined when the bond is located in the local region only by substituting the the directional distance $(u(y)-u(x))$ so that the local energy is equal to the nonlocal energy. This equality allows for the transition from one region of the decomposed domain to another, and creates the transitional region in the section of the domain determined by the chosen constant horizon.

By combining the two regions of energy, the quasi-nonlocal energy is

Definition 12. *One-dimensional Quasi-nonlocal Energy*

$$E_{QNL} = \frac{1}{2} \iint\limits_{x\leq 0 \cup y \leq 0} \gamma_\delta(|y-x|)(u(y)-u(x))^2 dydx + \frac{1}{2} \int\limits_{x<0} |u'(x)|^2 \omega_\delta(x) dx \tag{4.3}$$

where the weight function is given by

$$\omega_\delta(x) = \int_0^1 dt \int\limits_{|s|<\frac{x}{t}} |s|^2 \gamma(|s|) ds, \tag{4.4}$$

and the kernel $\gamma_\delta(x)$ is defined as

$$\begin{cases} \gamma_\delta(|x|) = \frac{1}{\delta^3}\gamma\left(\frac{|x|}{\delta}\right), \ \ \gamma \ \ \textit{is nonnegative and nonincreasing on} \ \ (0,1), \\ \textit{with supp}(\gamma) \subset [0,1] \ \textit{and} \int\limits_R |x|^2 \gamma(|x|) dx = 1. \end{cases}$$

Now we have a weight function that takes on the value of 0 in the nonlocal region, 1 in the local region, and a calculated value based on the kernels arrangement in the transtitional region. We can also conclude the following properties about the weight function.

Corollary 1. *Given the definition of the weight function as*

$$\omega_\delta(x) = \int_0^1 dt \int\limits_{|s|<\frac{x}{t}} |s|^2 \gamma(|s|) ds \tag{4.5}$$

then it is equivalent to

$$\omega_\delta(x) = 2\int_0^x s^2 \gamma_\delta(|s|) ds + 2x \int_x^\infty s\gamma_\delta(|s|) ds, \tag{4.6}$$

and its derivative is

$$\omega'_\delta(x) = 2\int_x^\infty s\gamma_\delta(s) ds. \tag{4.7}$$

Proof. By definition the weight function is

$$\omega_\delta(x) = \int_0^1 dt \int\limits_{|s|<\frac{x}{t}} |s|^2 \gamma(|s|) ds. \tag{4.8}$$

By symmetry of the absolute value

$$\int_0^1 dt \int\limits_{|s|<\frac{x}{t}} |s|^2 \gamma(|s|) ds = 2\int_0^1 dt \int_0^{\frac{x}{t}} s^2 \gamma_\delta(|s|) ds. \tag{4.9}$$

Then with careful restructuring, we find

$$\begin{aligned} 2\int_0^1 dt \int_0^{\frac{x}{t}} s^2 \gamma_\delta(|s|) ds &= 2\int_0^x s^2 \gamma_\delta(|s|) \int_0^1 dt ds + 2\int_x^\infty s^2 \gamma_\delta(|s|) \int_0^{\frac{x}{s}} dt ds \\ &= 2\int_0^x s^2 \gamma_\delta(|s|) ds + 2x\int_x^\infty s\gamma_\delta(|s|) ds. \end{aligned} \tag{4.10}$$

Therefore,

$$\omega_\delta(x) = 2\int_0^x s^2 \gamma_\delta(|s|) ds + 2x\int_x^\infty s\gamma_\delta(|s|) ds. \tag{4.11}$$

It is obvious from here that the derivative with respect to x of this definition of the weight function is

$$\omega'_\delta(x) = 2\int_x^\infty s\gamma_\delta(|s|) ds. \tag{4.12}$$

□

E_{QNL} is considered the energy space of the quasi-nonlocal coupling operator and the link between local and nonlocal energies is derived by taking the first variation of the quasi-nonlocal energy. The variation of the energy creates an operator to find the unique curve of shortest length connecting two points.

Theorem 10. *The variation of the combined local and nonlocal energies results is an operator that models the combination of nonlocal and local diffusion. This is known as the quasi-nonlocal operator, and is defined as*

$$\mathcal{L}^{QNL}u(x) = \begin{cases} 2\int\limits_{y\in R} \gamma_\delta(|y-x|)(u(y)-u(x))dy, \ \ \textit{if } x \le 0 \\ 2\int\limits_{y<0} \gamma_\delta(|y-x|)\Big(u(y)-u(x)\Big)dy + (\omega_\delta(x)u'(x))', \ \ \textit{if } x\in(0,\delta) \\ u''(x), \ \ \textit{if } x \ge \delta. \end{cases}$$

Proof. For any test function $v \in C^\infty(\Omega)$

$$\begin{aligned}
&\mathcal{L}^{QNL}(u) = \lim_{\epsilon\to 0}\frac{E^{QNL}(u+\epsilon v)-E^{QNL}(u)}{\epsilon} \\
=&\frac{1}{2}\lim_{\epsilon\to 0}\frac{\iint \gamma_\delta(|y-x|)(u(y)+\epsilon v(y)-u(x)-\epsilon v(x))^2dydx + \int \omega_\delta(x)|u'(x)+\epsilon v'(x)|^2dx}{\epsilon} \\
&-\frac{1}{2}\lim_{\epsilon\to 0}\frac{\iint \gamma_\delta(|y-x|)(u(y)-u(x))dydx + \int \omega_\delta(x)|u'(x)|^2dx}{\epsilon} \\
=&\iint \gamma_\delta(|y-x|)\big(u(x)v(x)-u(x)v(y)-u(y)v(x)+u(y)v(y)\big)dydx \\
&+\omega_\delta(x)u'(x)v(x)\Big|_0^1 - \int(\omega_\delta(x)u'(x))'v(x)dx \\
=&\iint \gamma_\delta(|y-x|)\big(2u(x)v(x)-2u(y)v(x)\big)dydx - \int(\omega_\delta(x)u'(x))'v(x)dx \\
=&-2\iint\limits_{x\le 0\cup y\le 0} \gamma_\delta(|y-x|)\big(u(y)-u(x)\big)v(x)dydx - \int\limits_{x>0}(\omega_\delta(x)u'(x))'v(x)dx
\end{aligned} \tag{4.13}$$

with assistance from symmetry, boundary conditions, definition of the weight function, and integration by parts. We can similarly define the operator for the nonlocal and local regions by taking the first variation of their energies. The results are the following

$$\begin{aligned}
\mathcal{L}^{QNL}(u) &= \lim_{\epsilon\to 0}\frac{E^{NL}(u+\epsilon v)-E^{NL}(u)}{\epsilon} \\
&= -2\int\limits_{y\in R}\gamma_\delta(|y-x|)(u(y)-u(x))v(x)dy,
\end{aligned} \tag{4.14}$$

and

$$\mathcal{L}^{QNL}(u) = \lim_{\epsilon \to 0} \frac{E^L(u+\epsilon v) - E^L(u)}{\epsilon}$$
$$= -(\omega_\delta(x)u'(x))'v(x) = -u''(x)v(x). \tag{4.15}$$

From here, the coupling operator is pieced together to describe the complete operator. These sections also must be adjusted so they reflect that in the diffusion process force is negative to the first variation of total energy. It can be concluded that the quasi-nonlocal coupling operator by regions is

- **Nonlocal Region**: $x \leq 0$

$$\mathcal{L}^{QNL}u(x) = 2 \int_{y \in R} \gamma_\delta(|y-x|)(u(y)-u(x))dy. \tag{4.16}$$

- **Transitional Region**: $0 < x \leq \delta$

$$\mathcal{L}^{QNL}u(x) = 2 \int_{y<0} \gamma_\delta(|y-x|)\big(u(y)-u(x)\big)dy + (\omega_\delta(x)u'(x))'. \tag{4.17}$$

- **Local Region**: $x \geq \delta$

$$\mathcal{L}^{QNL}u(x) = u''(x). \tag{4.18}$$

Grouped together as a piecewise function the quasi-nonlocal coupling operator

$$\mathcal{L}^{QNL}u(x) = \begin{cases} 2 \int_{y \in R} \gamma_\delta(|y-x|)(u(y)-u(x))dy, \text{ if } x \leq 0 \\ 2 \int_{y<0} \gamma_\delta(|y-x|)\Big(u(y)-u(x)\Big)dy + (\omega_\delta(x)u'(x))', \text{ if } x \in (0,\delta) \end{cases}$$ □

This is a continuum diffusion model that links local and nonlocal models seamlessly through

definitions as the first variation of total energy. This operator is self-adjoint meaning the forces acting on x from y are equivalent to the reverse. The balance of linear momentum is given by symmetry, and the flux balance and energy conservation are satisfied.

CHAPTER 5: FINITE DIFFERENCE SCHEME FOR QNL COUPLING

For the last decade, nonlocal integro-differential type models have been employed to describe physical systems. This is due to their natural ability to model physical phenomena at small scales and their reduced regularity requirements which lead to greater flexibility [3, 19, 4, 40, 10, 12, 13, 15, 16, 18, 20, 23, 24, 26, 31, 32, 35, 41]. These nonlocal models are defined through a length scale parameter δ, the horizon, which measures the extent of nonlocal interaction. An important feature of nonlocal models is that they restore the corresponding classical partial differential equation models as the horizon $\delta \to 0$ [12, 13].

Nonlocal models that are compatible with the local partial differential equations are often very computationally expensive and require additional attention to the boundary treatments since a layer of volumetric boundary conditions is needed within the physical system. Meanwhile, nonlocal models need less regularity requirements which helps the descriptions near defects and singularities. Consequently, tremendous efforts have been devoted to combining nonlocal and local methods to keep accuracy around the irregularity while retaining efficiency away from the singularity.(See the review paper [11] for the state-of-art.)

In [14], a quasi-nonlocal (QNL) coupling method was proposed to combine the nonlocal and local diffusion operators in a seamless way using the variational approach. The coupled operator is proved to preserve many mathematical and physical properties on the continuous level, including the symmetry of operator, the balance of linear momentum, and the maximum principle. However, it is not clear how to retain these desired properties with proper numerical discretization. We will now propose a new finite difference method which inherits all properties from the continuous case.

We recall that the linear local diffusion model in one-dimensional space can be written as

$$u_t(x,t) = u_{xx}(x,t) + f(x,t). \tag{5.1}$$

The corresponding counterpart in the nonlocal setting is the linear nonlocal diffusion model which reads

$$u_t(x,t) = \int_{-\delta}^{\delta} \gamma_\delta(s)\Big(u(x+s,t) - u(x,t)\Big)ds, \tag{5.2}$$

where $\gamma_\delta(s)$ denotes the isotropic nonlocal diffusion kernel satisfying the following assumption with $\gamma_\delta(\cdot)$ being a rescaled kernel,

$$\begin{cases} \gamma_\delta(|s|) = \dfrac{1}{\delta^3}\gamma\left(\dfrac{|s|}{\delta}\right), \quad \gamma \text{ is nonnegative and nonincreasing on (0,1),} \\ \text{with } \mathrm{supp}(\gamma) \subset [0,1] \text{ and } \displaystyle\int_{-\delta}^{\delta} |s|^2\gamma(|s|)ds = 2\,. \end{cases} \tag{5.3}$$

We will display more details about the coupling and numerical schemes in the following sections.

More precisely, we will organize the process as follows. In the first section we recall the energy-based quasi-nonlocal coupling from [14] to build the coupling operator $\mathcal{L}_\delta^{qnl}$ bridging the nonlocal and local diffusion problems and introduce space-time discretizations as well as the new finite difference method (FDM). In the next section, we estimate the consistency errors of the proposed scheme using Taylor expansions. The third section's focus is on proving the discrete maximum principle and hence, the stability of proposed scheme. In the next section, we combine the consistency and stability results to conclude the convergence estimates. Then we mathematically study the Courant-Friedrichs-Lewy (CFL) condition for the space-time discretization. In the final two sections, we test several benchmark examples to confirm our theoretical findings, and concluding results.

5.1 Discretized Quasi-Nonlocal Coupling

Now, we consider the domain to be $\Omega_\delta = [-1-\delta,\, 1]$, with the coupling interface of nonlocal and local models at $x^* = 0$; $(-1,\, 0)$ denotes the nonlocal region with nonlocal boundary layer at $[-1-\delta, -1]$ and $(0,\, 1)$ denotes the local region with local boundary point at $\{1\}$, as illustrated in Figure 5.1.

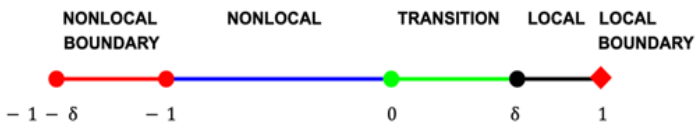

Figure 5.1: Partitioning and boundary layer for a discretized one dimensional domain.

In [14], the quasi-nonlocal operator $\mathcal{L}_\delta^{qnl} u(x,t)$ is introduced to smoothly bridge the local and nonlocal regions over the transitional region $[0,\, \delta]$. The corresponding coupled diffusion problem is proved to be a well-posed initial value problem and is given by

$$\begin{cases} u_t(x,t) = \mathcal{L}_\delta^{qnl} u(x,t) + f(x,t), & \text{for } \; T > t > 0 \;\text{ and }\; x \in (-1,1), \\ u(x,0) = u_0(x), & \text{for } \; x \in (-1,1), \\ u(x,t) = 0, & \text{for } \; x \in [-1-\delta, -1], \;\text{ or }\; x = 1. \end{cases} \tag{5.4}$$

$\mathcal{L}_\delta^{qnl}$ employed in equation (5.4) is the quasi-nonlocal coupling operator which describes the diffusion within the nonlocal, transitional, and local regions, respectively. The expression of

$\mathcal{L}_\delta^{qnl}$ is given below

$$\mathcal{L}_\delta^{qnl}u(x,t) = \begin{cases} \displaystyle\int_{-\delta}^{\delta}\Big(u(x+s,t)-u(x,t)\Big)\gamma_\delta(s)ds, & \text{if } x\in(-1,0), \\ \displaystyle\int_{x}^{\delta}\gamma_\delta(s)\Big(u(x-s,t)-u(x,t)\Big)ds+\Big(\int_{x}^{\delta}s\gamma_\delta(s)ds\Big)u_x(x,t) & \\ \quad+\Big(\displaystyle\int_0^x s^2\gamma_\delta(s)+x\int_x^\delta s\gamma_\delta(s)ds\Big)u_{xx}(x), & \text{if } x\in[0,\delta], \\ u_{xx}(x,t), & \text{if } x\in(\delta,1). \end{cases} \tag{5.5}$$

Next, we discuss the numerical settings for the spatial and temporal discretization. We use u_i^n to denote the numerical approximation of the exact solution $u(x_i,t^n)$ with spatial and temporal step sizes being with $\Delta x := \frac{1}{N}$ and $\Delta t := \frac{T}{N_T}$, respectively. Hence, the spatial grid is x_i and temporal grid is $t_n = n\Delta t$. For simplicity, we drop x and t but only use i and n accordingly. The relation between Δx and Δt will be determined later by the CFL condition. Meanwhile, we assume that the horizon δ is a multiple of Δx with $\delta = r\Delta x$ and $r\in\mathbb{N}$.

Recall that the entire computational domain is $\Omega_\delta := [-1-\delta,\,1]$, so the interior domain is $\Omega = [-1,1]$ with interface at $x^* = 0$; the volumetric boundary layer for the nonlocal region is $\Omega_n = [-1-\delta,-1)$; and the local boundary point is $\Omega_c = \{1\}$. Next we denote the set of spatial grids by I and $I = I_\Omega \cup I_{\Omega_n} \cup I_{\Omega_c}$, where $I_\Omega = \{1,2,...,2N-1\}$ denotes the interior grids, $I_{\Omega_n} = \{-(r-1),...,0\}$ denotes the nonlocal volumetric boundary grids, and $I_{\Omega_c} = \{2N\}$ denotes the local boundary point.

Following the scope of asymptotically compatible schemes [43, 44], we define the spatial discretization of the quasi-nonlocal coupling operator $\mathcal{L}_{\delta,\Delta x}^{qnl}$ as follows.

Definition 13. *Discretized Quasi-nonlocal Coupling Operator*

$$\mathcal{L}^{qnl}_{\delta,\Delta x}u^n_i := \begin{cases} \displaystyle\sum_{j=1}^{r} \frac{u^n_{i+j}-2u^n_i+u^n_{i-j}}{(j\Delta x)^2}\int_{(j-1)\Delta x}^{j\Delta x} s^2\gamma_\delta(s)ds, & \text{if } x_i \le 0, \\ \displaystyle\sum_{j=\frac{x_i}{\Delta x}+1}^{r} \frac{u^n_{i+j-1}-2u^n_i+u^n_{i-j+1}}{2(j-1)\Delta x}\int_{(j-1)\Delta x}^{j\Delta x} s\gamma_\delta(s)ds \\ \quad - \displaystyle\sum_{j=\frac{x_i}{\Delta x}+1}^{r} \frac{u^n_{i+j-1}-u^n_{i-j+1}}{2(j-1)\Delta x}\int_{(j-1)\Delta x}^{j\Delta x} s\gamma_\delta(s)ds \\ \quad + \left(\displaystyle\int_{x_i}^{\delta} s\gamma_\delta(s)ds\right)\frac{u^n_{i+1}-u^n_i}{\Delta x} \\ \quad + \left(\displaystyle\int_0^{x_i} s^2\gamma_\delta(s)ds + x_i\int_{x_i}^{\delta} s\gamma_\delta(s)ds\right)\frac{u^n_{i+1}-2u^n_i+u^n_{i-1}}{(\Delta x)^2}, & \text{if } x_i \in (0,\delta], \\ \dfrac{u^n_{i+1}-2u^n_i+u^n_{i-1}}{(\Delta x)^2}, & \text{if } x_i \in (\delta,1). \end{cases} \tag{5.6}$$

For the temporal discretization, we employ the simplest explicit Euler scheme due to the limitation of first order accuracy in the spatial discrezation, which will be proved later. Hence the full finite difference method discretization of (5.4) is

$$\frac{u^{n+1}_i-u^n_i}{\Delta t} = \mathcal{L}^{qnl}_{\delta,\Delta x}u^n_i + f^n_i, \quad i \in I_\Omega, \tag{5.7}$$

where $f^n_i = f(x_i, t^n)$.

Figure 5.2 displays a sampling set of spatial stencils using $N = 5$ on domain $[-1-\delta, 1]$. The step size is $\Delta x = \frac{1}{5}$ and the horizon $\delta = r\Delta x$ with $r = 3$.

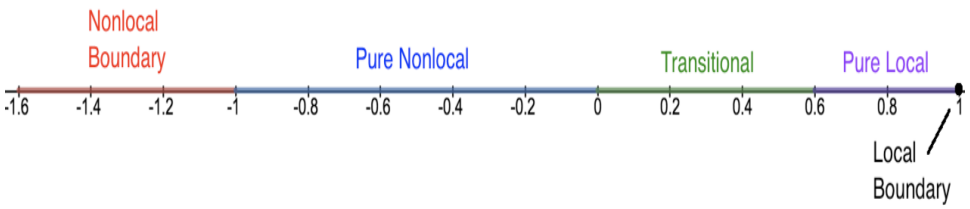

Figure 5.2: Example finite difference stencil with $\Delta x = \frac{1}{5}$, horizon $\delta = r\Delta x$, and $r = 3$.

Remark 1. *In [14], the time-integral is still approximated by the explicit Euler method, and the* $\tilde{\mathcal{L}}^{qnl}_{\delta,\Delta x}$ *is approximated by the following finite difference scheme given the interface at* $x^* = 0$*:*

$$\tilde{\mathcal{L}}^{qnl}_{\delta,\Delta x} u_i^n \approx \begin{cases} 2\displaystyle\sum_{j=1}^{r} \frac{u_{i+j}^n - 2u_i^n + u_{i-j}^n}{(j\Delta x)^2} \int_{(j-1)\Delta x}^{j\Delta x} s^2 \gamma_\delta(s) ds, & \text{if } x_i \le 0. \\ \displaystyle\sum_{j=\frac{x_i}{\Delta x}}^{r} \frac{u_{i+j}^n - 2u_i^n + u_{i-j}^n}{(j\Delta x)^2} \int_{(j-1)\Delta x}^{j\Delta x} s^2 \gamma_\delta(s) ds \\ \quad - \displaystyle\sum_{j=\frac{x_i}{\Delta x}}^{r} \frac{u_{i+j}^n - u_{i-j}^n}{j\Delta x} \int_{(j-1)\Delta x}^{j\Delta x} s\gamma_\delta(s) ds \\ \quad + 2\left(\displaystyle\int_{x_i}^{\delta} s\gamma_\delta(s) ds \right) \frac{u_{i+1}^n - u_i^n}{\Delta x} \\ \quad + \left(2\displaystyle\int_0^{x_i} s^2 \gamma_\delta(s) ds + 2x_i \int_{x_i}^{\delta} s\gamma_\delta(s) ds \right) \frac{u_{i+1}^n - 2u_i^n + u_{i-1}^n}{(\Delta x)^2}, & \text{if } x_i \in (0, \delta], \\ \dfrac{u_{i+1}^n - 2u_i^n + u_{i-1}^n}{(\Delta x)^2}, & \text{if } x_i \in (\delta, 1). \end{cases} \tag{5.8}$$

Comparing (5.6) *with* (5.8)*, we notice that the difference is replacing* j *in the original scheme by* $(j-1)$ *in the new scheme. This is the main difference in the approximation that allows the equation* (5.6) *to satisfy the discrete maximum principle whereas equation* (5.8) *does not. We will rigorously prove this in Section 5.3.*

Remark 2. *For numerical schemes that preserve the maximum principles in high dimensional space there are other types of coupling methods developed for two-dimensional problems. [45, 48] These coupling schemes are based on a domain-decomposition methods via Neumann or Robin type boundary conditions, and are rigorously proved to keep the maximum principles.*

Regarding the conservation of flux, notice that the operator $\mathcal{L}^{qnl}_{\delta,\Delta x}$ of new scheme (5.6) *is symmetric, hence, it possesses this property. In general, one has to keep interaction symmetries across the transitional region of the coupling region. However, the nonlocal neighborhood, $B_\delta(x)$, becomes a disk (in two dimensions) or a ball (in three dimensions), making the intersections with the interface more complex. As a result, it is not easy to preserve the flux in higher dimensions.*

5.2 Consistency of the Discretized Quasi-Nonlocal Operator

In this section, we estimate the consistency error of the scheme (5.7) with $\mathcal{L}^{qnl}_{\delta,\Delta x}$ defined in (5.6).

Theorem 11. *Let the horizon $\delta = r\Delta x$ with $r \in \mathbb{N}$ being fixed, and suppose $u(x,t)$ is the strong solution to* (5.4)*, and u_i^n is the discrete solution to the scheme* (5.7) *with $i \in I_\Omega$ and $t^n = n\Delta t$. Also assume that the exact solution u is sufficiently smooth, specifically $u(x,t) \in C^4([-1-\delta, 1]\times[0,T])$. Suppose at any given time level $t^n = n\Delta t$ we have $u(x_i, t^n) = u_i^n$, $\forall i \in I_\Omega = \{1,\dots,2N-1\}$, then for the next time level $n+1$ the consistency error of the scheme satisfies*

$$|u_i^{n+1} - u(x_i, t^{n+1})| \le C_\delta \Delta t \left((\Delta x) + (\Delta t)\right), \ \forall i = 1,\dots,2N-1, \tag{5.9}$$

where C_δ is a constant independent of Δx and Δt.

Proof. We evolve $u(x_i, t^n)$ and u_i^n by one time step Δt according to three differential regions.

Local: If $x_i > \delta$ or simply $i \in \{N+r+1, ..., 2N-1\}$, then the continuous and discrete

equations follow the expressions in the local region. So at (x_i, t^n), we have the continuous equation:

$$u_t(x_i, t_n) = u_{xx}(x_i, t_n) + f(x_i, t_n), \tag{5.10}$$

and the discrete equation:

$$\frac{u_i^{n+1} - u_i^n}{\Delta t} = \frac{u_{i+1}^n - 2u_i^n + u_{i-1}^n}{(\Delta x)^2} + f_i^n \tag{5.11}$$

with $f_i^n = f(x_i, t^n)$.

Notice from the consistency assumption that $u_i^n = u(x_i, t^n)$, so we can rewrite the discrete equation as

$$\frac{u_i^{n+1} - u(x_i, t^n)}{\Delta t} = \frac{u(x_{i+1}, t^n) - 2u(x_i, t^n) + u(x_{i-1}, t^n)}{(\Delta x)^2} + f(x_i, t^n). \tag{5.12}$$

We apply the Taylor expansion at the spatial grid (x_i) up to the fourth-order derivative and obtain an estimate of u_i^{n+1}, which is

$$\begin{aligned} u_i^{n+1} =& u(x_i, t^n) + \Delta t \left(\frac{u(x_{i+1}, t^n) - 2u(x_i, t^n) + u(x_{i-1}, t^n)}{(\Delta x)^2} + f(x_i, t^n) \right) \\ =& u(x_i, t^n) + \Delta t \left(\frac{(\Delta x)^2 u_{xx}(x_i, t^n) + O(\Delta x^4)}{(\Delta x)^2} + f(x_i, t^n) \right) \\ =& u(x_i, t^n) + \Delta t \Big(u_{xx}(x_i, t^n) + f(x_i, t^n) \Big) + O\big(\Delta t (\Delta x)^2\big). \end{aligned} \tag{5.13}$$

Now, let us estimate the continuous solution $u(x_i, t^{n+1})$. This time, we apply the Taylor expansion at the time grid (t^n) and get

$$\begin{aligned} u(x_i, t^{n+1}) =& u(x_i, t^n) + \Delta t u_t(x_i, t^n) + O(\Delta t^2) \\ =& u(x_i, t^n) + \Delta t \Big[\big(u_{xx}(x_i, t^n) + f(x_i, t^n) \big) \Big] + O(\Delta t^2), \end{aligned} \tag{5.14}$$

where we substitute $u_t(x_i, t^n)$ by the continuous equation on the local region.

By subtracting (5.13) from (5.14) we obtain

$$u_i^{n+1} - u(x_i, t^{n+1}) = O\big(\Delta t(\Delta x)^2\big) + O\big((\Delta t)^2\big). \tag{5.15}$$

Nonlocal: Next we consider the fully nonlocal region where $x_i \leq 0$ or simply $i \in \{1, \ldots, N\}$. We first have the continuous equation:

$$\begin{aligned}
u_t(x_i, t^n) &= \int_{-\delta}^{\delta} \gamma_\delta(s)\Big(u(x_i + s, t^n) - u(x_i, t^n)\Big)ds + f(x_i, t^n) \\
&= \int_{-\delta}^{0} \gamma_\delta(s)\Big(u(x_i + s, t^n) - u(x_i, t^n)\Big)ds \\
&\quad + \int_{0}^{\delta} \gamma_\delta(s)\Big(u(x_i + s, t^n) - u(x_i, t^n)\Big)ds + f(x_i, t^n) \\
&= \int_{0}^{\delta} \gamma_\delta(-s)\Big(u(x_i - s, t^n) - u(x_i, t^n)\Big)ds \\
&\quad + \int_{0}^{\delta} \gamma_\delta(s)\Big(u(x_i + s, t^n) - u(x_i, t^n)\Big)ds + f(x_i, t^n).
\end{aligned} \tag{5.16}$$

Because of the isotropic property of the nonlocal kernel $\gamma_\delta(s)$ summarized in (5.3), we have

$$u_t(x_i, t^n) = \int_{0}^{\delta} \gamma_\delta(s)\Big(u(x_i + s, t^n) - 2u(x_i, t^n) + u(x_i - s, t^n)\Big)ds + f(x_i, t^n). \tag{5.17}$$

Clearly, we can divide the integral into the sum of subintegrals on the union of subintervals, so we have,

$$u_t(x_i, t^n) = \sum_{j=1}^{r} \int_{(j-1)\Delta x}^{j\Delta x} \gamma_\delta(s)\Big(u(x_i + s, t^n) - 2u(x_i, t^n) + u(x_i - s, t^n)\Big)ds + f(x_i, t^n). \tag{5.18}$$

Meanwhile, we have the discrete equation to advance u_i^n to u_i^{n+1}:

$$\frac{u_i^{n+1} - u_i^n}{\Delta t} = \sum_{j=1}^{r} \frac{u_{i+j}^n - 2u_i^n + u_{i-j}^n}{(j\Delta x)^2} \int_{(j-1)\Delta x}^{j\Delta x} s^2 \gamma_\delta(s) ds + f_i^n. \tag{5.19}$$

This gives,

$$u_i^{n+1} = u_i^n + \Delta t\Bigg(\sum_{j=1}^{r} \frac{u_{i+j}^n - 2u_i^n + u_{i-j}^n}{(j\Delta x)^2} \int_{(j-1)\Delta x}^{j\Delta x} s^2 \gamma_\delta(s) ds + f_i^n \Bigg). \tag{5.20}$$

Now we want to estimate the continuous solution $u(x_i, t^{n+1})$. We know that

$$u(x_i, t^{n+1}) = u(x_i, t^n) + \Delta t u_t(x_i, t^n) + O(\Delta t^2). \tag{5.21}$$

Hence, inserting the continuous description of the nonlocal diffusion, (5.18), we obtain

$$\begin{aligned} u(x_i,t^{n+1}) &= u(x_i, t^n) + \Delta t u_t(x_i, t^n) + O(\Delta t^2) \\ &= u(x_i, t^n) + \Delta t \Bigg[\sum_{j=1}^{r} \int_{(j-1)\Delta x}^{j\Delta x} \gamma_\delta(s) s^2 \Bigg(\frac{u(x_i + s, t^n) - 2u(x_i, t^n) + u(x_i - s, t^n)}{s^2} \Bigg) ds \\ &\quad + f(x_i, t^n) \Bigg] + O(\Delta t^2) \end{aligned} \tag{5.22}$$

for each integral term from $[(j-1)\Delta x,\, j\Delta x]$ within the summation. We then focus on the fractional term and apply a Taylor expansion to $u(x_i + s, t^n)$ and $u(x_i - s, t^n)$ for s at $(j\Delta x)$ up to a fourth-order derivative. This gives an estimate of

$$\begin{aligned} u(x_i,t^{n+1}) &= u(x_i, t^n) \\ &\quad + \Delta t \Bigg[\sum_{j=1}^{r} \int_{(j-1)\Delta x}^{j\Delta x} \gamma_\delta(s) s^2 \frac{1}{(j\Delta x)^2} \Bigg(\Big(u(x_{i+j}, t^n) - 2u(x_i, t^n) + u(x_{i-j}, t^n) \Big) + O(s^4) \Bigg) ds \\ &\quad + f(x_i, t^n) \Bigg] + O(\Delta t^2) \\ &= u_i^n + \Delta t \Bigg[\sum_{j=1}^{r} \int_{(j-1)\Delta x}^{j\Delta x} \gamma_\delta(s) s^2 \frac{1}{(j\Delta x)^2} \Bigg(\Big(u_{i+j}^n - 2u_i^n + u_{i-j}^n \Big) \Bigg) ds + O(\Delta x^2) \\ &\quad + f(x_i, t^n) \Bigg] + O(\Delta t^2). \end{aligned} \tag{5.23}$$

Then by subtracting (5.20) from (5.23), we can get

$$u_i^{n+1} - u(x_i, t^{n+1}) = O(\Delta t) \cdot O(\Delta x)^2 + O(\Delta t^2). \tag{5.24}$$

Transitional: Finally we consider when $x_i \in (0,\, \delta]$ or equivalently $i \in \{N+1, \ldots, N+r\}$, and again we will look at the continuous equation for the time derivative $u_t(x_i, t^n)$ first.

$$\begin{aligned} u_t(x_i, t^n) = \Bigg[\int_{x_i}^{\delta} \gamma_\delta(s) \Big(u(x_i - s, t^n) - u(x_i, t^n) \Big) ds + \left(\int_{x_i}^{\delta} s\gamma_\delta(s) ds \right) u_x(x_i, t^n) \\ + \left(\int_0^{x_i} s^2 \gamma_\delta(s) ds + x_i \int_{x_i}^{\delta} s\gamma_\delta(s) ds \right) u_{xx}(x_i, t^n) \Bigg] + f(x_i, t^n), \end{aligned} \tag{5.25}$$

and splitting and symmetrizing the first integral gives

$$\begin{aligned} u_t(x_i, t^n) = \int_{x_i}^{\delta} \frac{\gamma_\delta(s)}{2} \Big(u(x_i - s, t^n) - 2u(x_i, t^n) + u(x_i + s, t^n) \Big) ds \\ + \int_{x_i}^{\delta} \frac{\gamma_\delta(s)}{2} \Big(u(x_i - s, t^n) - u(x_i + s, t^n) \Big) ds + \left(\int_{x_i}^{\delta} s\gamma_\delta(s) ds \right) u_x(x_i, t^n) \\ + \left(\int_0^{x_i} s^2 \gamma_\delta(s) ds + x_i \int_{x_i}^{\delta} s\gamma_\delta(s) ds \right) u_{xx}(x_i, t^n) + f(x_i, t^n), \end{aligned} \tag{5.26}$$

and dividing these two integrals into the sum of subintegrals on the union of subintervals, and modifing each integrand in the scope of thr asymptotically compatible scheme [44], we find

$$\begin{aligned} u_t(x_i,t^n) = \sum_{j=\frac{x_i}{\Delta x}+1}^{r} \int_{(j-1)\Delta x}^{j\Delta x} \frac{\gamma_\delta(s)s}{2} \left(\frac{u(x_i - s, t^n) - 2u(x_i, t^n) + u(x_i + s, t^n)}{s} \right) ds \\ + \sum_{j=\frac{x_i}{\Delta x}+1}^{r} \int_{(j-1)\Delta x}^{j\Delta x} \frac{\gamma_\delta(s)s}{2} \left(\frac{u(x_i - s, t^n) - u(x_i + s, t^n)}{s} \right) ds + \left(\int_{x_i}^{\delta} s\gamma_\delta(s) ds \right) u_x(x_i, t^n) \\ + \left(\int_0^{x_i} s^2 \gamma_\delta(s) ds + x_i \int_{x_i}^{\delta} s\gamma_\delta(s) ds \right) u_{xx}(x_i, t^n) + f(x_i, t^n). \end{aligned} \tag{5.27}$$

Now working with the discrete equation for u_i^{n+1}

$$\begin{aligned}\frac{u_i^{n+1}-u_i^n}{\Delta t} &= \sum_{j=\frac{x_i}{\Delta x}+1}^{r} \frac{u_{i+j-1}^n - 2u_i^n + u_{i-j+1}^n}{2(j-1)\Delta x}\int_{(j-1)\Delta x}^{j\Delta x} s\gamma_\delta(s)ds \\ &- \sum_{j=\frac{x_i}{\Delta x}+1}^{r} \frac{u_{i+j-1}^n - u_{i-j+1}^n}{2(j-1)\Delta x}\int_{(j-1)\Delta x}^{j\Delta x} s\gamma_\delta(s)ds + \left(\int_{x_i}^{\delta} s\gamma_\delta(s)ds\right)\frac{u_{i+1}^n - u_i^n}{\Delta x} \\ &+ \left(\int_0^{x_i} s^2\gamma_\delta(s)ds + x_i\int_{x_i}^{\delta} s\gamma_\delta(s)ds\right)\frac{u_{i+1}^n - 2u_i^n + u_{i-1}^n}{(\Delta x)^2} + f_i^n. \end{aligned} \tag{5.28}$$

This gives,

$$\begin{aligned}u_i^{n+1} &= u_i^n + \Delta t\Bigg[\sum_{j=\frac{x_i}{\Delta x}+1}^{r} \frac{u_{i+j-1}^n - 2u_i^n + u_{i-j+1}^n}{2(j-1)\Delta x}\int_{(j-1)\Delta x}^{j\Delta x} s\gamma_\delta(s)ds \\ &- \sum_{j=\frac{x_i}{\Delta x}+1}^{r} \frac{u_{i+j-1}^n - u_{i-j+1}^n}{2(j-1)\Delta x}\int_{(j-1)\Delta x}^{j\Delta x} s\gamma_\delta(s)ds + \left(\int_{x_i}^{\delta} s\gamma_\delta(s)ds\right)\frac{u_{i+1}^n - u_i^n}{\Delta x} \\ &+ \left(\int_0^{x_i} s^2\gamma_\delta(s)ds + x_i\int_{x_i}^{\delta} s\gamma_\delta(s)ds\right)\frac{u_{i+1}^n - 2u_i^n + u_{i-1}^n}{(\Delta x)^2} + f_i^n\Bigg]. \end{aligned} \tag{5.29}$$

Again we want to estimate difference between $u(x_i, t^{n+1})$ and u_i^{n+1}.

For each integral term $[(j-1)\Delta x, j\Delta x]$ within the summation of (5.27), we then use a Taylor expansion for $u(x_i + s, t^n)$ and $u(x_i - s, t^n)$ for s at $(j-1)\Delta x$, which is similar to the processing we did for the nonlocal region.

$$
\begin{aligned}
u(x_i, t^{n+1}) &= u(x_i, t^n) \\
&+ \Delta t \Bigg[\sum_{j=\frac{x_i}{\Delta x}+1}^{r} \int_{(j-1)\Delta x}^{j\Delta x} \frac{\gamma_\delta(s)s}{2(j-1)\Delta x} \Big(u(x_{i+j-1}, t^n) - 2u(x_i, t^n) + u(x_{i-j+1}, t^n) + O(s^2) \Big) ds \\
&+ \sum_{j=\frac{x_i}{\Delta x}+1}^{r} \int_{(j-1)\Delta x}^{j\Delta x} \frac{\gamma_\delta(s)s}{2(j-1)\Delta x} \Big(u(x_{i+j-1}, t^n) - u(x_{i-j+1}, t^n) + O(s) \Big) ds \\
&+ \left(\int_{x_i}^{\delta} s\gamma_\delta(s) ds \right) \left(\frac{u(x_{i+1}, t^n) - (x_i, t^n)}{\Delta x} + O(\Delta x) \right) \\
&+ \left(\int_0^{x_i} s^2 \gamma_\delta(s) ds + x_i \int_{x_i}^{\delta} s\gamma_\delta(s) ds \right) \left(\frac{u_(x_{i+1}, t^n) - 2_(x_i, t^n) +_(x_{i-1}, t^n)}{\Delta x^2} + O(\Delta x^2) \right) \\
&+ f(x_i, t^n) \Bigg] + O(\Delta t^2). \qquad (5.30)
\end{aligned}
$$

By subtracting (5.29) from (5.30) we have

$$
u_i^{n+1} - u(x_i, t^{n+1}) = O(\Delta t) O(\Delta x) + O(\Delta t^2). \qquad (5.31)
$$

Therefore, $\|u(x_i, t^{n+1}) - u_i^{n+1}\|_{L^\infty} = O(\Delta t) O(\Delta x) + O(\Delta t^2)$ with the highest restrictions from the transitional region. Since the order of accuracy is greater than zero, the finite difference scheme is consistent. □

5.3 Stability of the Discretized Quasi-nonlocal Operator

Global stability of the scheme is attained by the discrete maximum principle. To prove the discrete maximum principle for the quasi-nonlocal coupling equation with an underlying finite difference discretization the spatial operator $(-\mathcal{L}_{\delta,\Delta x}^{qnl})$ must be positive-definite, and the time discretization, that is a single explicit Euler integrator, must be a convex scheme. Recall the interior domain $\Omega = [-1, 1]$ with interface at $x^* = 0$. The volumetric boundary layer for the nonlocal region is $\Omega_n = (-1-\delta, -1]$, and the local boundary point is $\Omega_c = \{1\}$. The corresponding sets of spatial grids are $I_\Omega = \{1, 2, ..., 2N-1\}$ for Ω, $I_{\Omega_n} = \{-(r-1), ..., 0\}$

for Ω_n, and $I_{\Omega_c} = \{2N\}$ for Ω_c. Let $I = I_\Omega \cup I_{\Omega_n} \cup I_{\Omega_c}$ denote the union of total stencils within the entire domain (Interior and Boundary), and $I_B = I_{\Omega_n} \cup I_{\Omega_c}$ denote the stencils within the boundary regions $\Omega_n \cup \Omega_c$ (Boundary).

Next we will prove the positive-definiteness of $(-\mathcal{L}^{qnl}_{\delta,\Delta x})$ in Theorem 12, which is the discrete maximum principle for the static case; and then extend the result to the dynamic case in Theorem 13 where the time derivative is involved.

Theorem 12. ***Discrete Maximum Principle for the Static Case*** *The discrete operator $\mathcal{L}^{qnl}_{\delta,\Delta x}$ satisfies the maximum principle. For $u(x_i) \in \ell^1(I)$ with $\left(-\mathcal{L}^{qnl}_{\delta,\Delta x}\right)(u(x_j)) \leq 0$ and $j \in I_\Omega$, and for any $i \in I = I_\Omega \cup I_B$, we have*

$$\max_{i\in I} u(x_i) \leq \max_{i\in I_B} u(x_i). \tag{5.32}$$

Furthermore, equality holds, and $u(x_i)$ is a constant function on stencils I.

Proof. Suppose the discrete function u achieves its strictly maximum values at an interior grid $j^* \in I_\Omega$.

Case I Nonlocal: Consider $j^* \in \{1, 2, ..., N\}$. Then since $u(x_{j^*})$ is a strict maximum

$$\mathcal{L}^{qnl}_{\delta,\Delta x} u_h(x_{j^*}) = \sum_{k=1}^{r} \frac{u(x_{j^*+k}) - 2u(x_{j^*}) + u(x_{j^*-k})}{(k\Delta x)^2} \int_{(k-1)\Delta x}^{k\Delta x} s^2 \gamma_\delta(s) ds < 0 \tag{5.33}$$

which contradicts $-\mathcal{L}^{qnl}_{\delta,\Delta x} u(x^*_j) \leq 0$ unless u is constant.

Case II Transitional: Consider $j^* \in \{N+1, N+2, ..., N+r\}$. We observe that

$$\int_{(k-1)\Delta x}^{k\Delta x} s^2 \gamma_\delta(s) ds > (k-1)\Delta x \int_{(k-1)\Delta x}^{k\Delta x} s\gamma_\delta(s) ds. \tag{5.34}$$

Using $u(x_{j^*})$

$$\begin{aligned}\mathcal{L}^{qnl}_{\delta,\Delta x}u_h(x_{j^*}) = &\sum_{k=\frac{x_{j^*}}{\Delta x}+1}^{r} \frac{u(x_{j^*+k-1}) - 2u(x_{j^*}) + u(x_{j^*-k+1})}{2(k-1)^2(\Delta x)^2}\int_{(k-1)\Delta x}^{k\Delta x} s^2\gamma_\delta(s)ds \\ &- \sum_{k=\frac{x_{j^*}}{\Delta x}+1}^{r} \frac{u(x_{j^*+k-1}) - u(x_{j^*-k+1})}{2(k-1)\Delta x}\int_{(k-1)\Delta x}^{k\Delta x} s\gamma_\delta(s)ds \\ &+ \left(\int_{x_{j^*}}^{\delta} s\gamma_\delta(s)ds\right)\frac{u(x_{j^*+1}) - u(x_{j^*})}{\Delta x} \\ &+ \left(\int_0^{x_j^*} s^2\gamma_\delta(s)ds + x_{j^*}\int_{x_{j^*}}^{\delta} s\gamma_\delta(s)ds\right)\frac{u(x_{j^*+1}) - 2u(x_{j^*}) + u(x_{j^*-1})}{(\Delta x)^2}. \quad (5.35)\end{aligned}$$

Also since $u(x_{j^*})$ is a strict maximum we know

$$\frac{u(x_{j^*+k-1}) - 2u(x_{j^*}) + u(x_{j^*-k+1})}{2(k-1)^2(\Delta x)^2} < 0, \quad (5.36)$$

and combined with (5.34), this gives

$$\begin{aligned}\mathcal{L}^{qnl}_{\delta,\Delta x}u(x_{j^*}) \le &\sum_{k=\frac{x_{j^*}}{\Delta x}+1}^{r} \frac{u(x_{j^*+k-1}) - 2u(x_{j^*}) + u(x_{j^*-k+1})}{2(k-1)^2(\Delta x)^2}\cdot(k-1)\Delta x\int_{(k-1)\Delta x}^{k\Delta x} s\gamma_\delta(s)ds \\ &- \sum_{k=\frac{x_{j^*}}{\Delta x}+1}^{r} \frac{u(x_{j^*+k-1}) - u(x_{j^*-k+1})}{2(k-1)\Delta x}\int_{(k-1)\Delta x}^{k\Delta x} s\gamma_\delta(s)ds \\ &+ \left(\int_{x_{j^*}}^{\delta} s\gamma_\delta(s)ds\right)\frac{u(x_{j^*+1}) - u(x_{j^*})}{\Delta x} \\ &+ \left(\int_0^{x_j^*} s^2\gamma_\delta(s)ds + x_{j^*}\int_{x_{j^*}}^{\delta} s\gamma_\delta(s)ds\right)\frac{u(x_{j^*+1}) - 2u(x_{j^*}) + u(x_{j^*-1})}{(\Delta x)^2}. \quad (5.37)\end{aligned}$$

Simplifying we conclude

$$\begin{aligned}\mathcal{L}^{qnl}_{\delta,\Delta x}u_h(x_{j^*}) \leq & \sum_{k=\frac{x_{j^*}}{\Delta x}+1}^{r} \frac{-2u(x_{j^*})+2u(x_{j^*-k+1})}{2(k-1)\Delta x}\int_{(k-1)\Delta x}^{k\Delta x} s\gamma_\delta(s)ds \\ & + \left(\int_{x_{j^*}}^{\delta} s\gamma_\delta(s)ds\right)\frac{u(x_{j^*+1})-u(x_{j^*})}{\Delta x} \\ & + \left(\int_0^{x_j^*} s^2\gamma_\delta(s)ds + x_{j^*}\int_{x_{j^*}}^{\delta} s\gamma_\delta(s)ds\right)\frac{u(x_{j^*+1})-2u(x_{j^*})+u(x_{j^*-1})}{(\Delta x)^2} < 0.\end{aligned} \tag{5.38}$$

which contradicts $-\mathcal{L}^{qnl}_{\delta,\Delta x}u(x_j) \leq 0$.

Case III Local: Consider $j^* \in \{N+r+1, ..., 2N-1\}$. Then since $u(x_{j^*})$ is a strict maximum

$$\mathcal{L}^{qnl}_{\delta,\Delta x}u(x_{j^*}) = \frac{u(x_{j^*+1})-2u(x_{j^*})+u(x_{j^*-1})}{(\Delta x)^2} < 0 \tag{5.39}$$

which contradicts $-\mathcal{L}^{qnl}_{\delta,\Delta x}u(x_j) \leq 0$. □

Next, we will consider the time-dependent case.

Theorem 13. ***Discrete Maximum Principle for the dynamic case*** *Suppose for $i \in I = I_\Omega \cup I_B$ and $n = 0, 1, ..., N_T - 1$ with $T = N_T \cdot \Delta t$ that $\{u_i^n\}$ solves the following discrete quasi-nonlocal diffusion equation.*

$$\begin{cases} \frac{u_i^{n+1}-u_i^n}{\Delta t} = \mathcal{L}^{qnl}_{\delta,\Delta x}u_i^n + f_i^n, \quad for\ i \in I_\Omega,\ and\ N_T > n \geq 0, \\ u_i^0 = g_i^0, \quad for\ i \in I\ (Initial\ Condition), \\ u_i^n = q_i^n, \quad for\ i \in I_B,\ n \geq 0\ (Boundary\ Condition), \end{cases} \tag{5.40}$$

then u_i^n satisfies the discrete maximum principle

$$u_i^n \leq \max\{g_i^0|_{i\in I}, \quad q_i^n|_{i\in I_B, n\geq 0}\} \tag{5.41}$$

given that $f_i^n \leq 0$ *for all* $i \in I_\Omega$*, all* $n \geq 0$*, and* $\frac{\Delta t}{\Delta x^2} \leq \frac{1}{4}$.

Proof. We denote $M = \max\{g_i^0|_{i\in I}, \quad q_i^n|_{i\in I_B, n\geq 0}\}$. Clearly, at $n = 0$ we have $u_i^0 \leq M$ for all $i \in I = I_\Omega \cup I_B$. We assume that this holds for $n = m$ with $0 \leq m \leq N_T - 2$. Now we would like to advance it to the next time level $n = m + 1$.

Case I Nonlocal: Consider $i \in \{1, 2, ..., N\}$ which is the nonlocal region. Then

$$\begin{aligned} u_i^{m+1} &= u_i^m + \Delta t\left(\mathcal{L}_{\delta,\Delta x}^{qnl} u_i^m + f_i^m\right) \\ &\leq u_i^m + \Delta t \mathcal{L}_{\delta,\Delta x}^{qnl} u_i^m \\ &= \left(1 - \frac{2\Delta t}{\Delta x^2}\sum_{k=1}^{r}\frac{1}{k^2}\int_{(k-1)\Delta x}^{k\Delta x} s^2\gamma_\delta(s)ds\right)u_i^m + \frac{\Delta t}{\Delta x^2}\sum_{k=1}^{r}\frac{u_{i+k}^m + u_{i-k}^m}{k^2}\int_{(k-1)\Delta x}^{k\Delta x} s^2\gamma_\delta(s)ds. \end{aligned}$$

Notice that

$$\sum_{k=1}^{r}\frac{1}{k^2}\int_{(k-1)\Delta x}^{k\Delta x} s^2\gamma_\delta(s)ds \leq \sum_{k=1}^{r}\int_{(k-1)\Delta x}^{k\Delta x} s^2\gamma_\delta(s)ds = \int_0^\delta s^2\gamma_\delta(s)ds = 1 \tag{5.42}$$

and $\dfrac{\Delta t}{\Delta x^2} \leq \dfrac{1}{4}$, so

$$\left(1 - \frac{2\Delta t}{\Delta x^2}\sum_{k=1}^{r}\frac{1}{k^2}\int_{(k-1)\Delta x}^{k\Delta x} s^2\gamma_\delta(s)ds\right) \geq 0. \tag{5.43}$$

Hence,

$$\begin{aligned} u_i^{m+1} &\leq \left(1 - \frac{2\Delta t}{\Delta x^2}\sum_{k=1}^{r}\frac{1}{k^2}\int_{(k-1)\Delta x}^{k\Delta x} s^2\gamma_\delta(s)ds\right)u_i^m + \frac{\Delta t}{\Delta x^2}\sum_{k=1}^{r}\frac{u_{i+k}^m + u_{i-k}^m}{k^2}\int_{(k-1)\Delta x}^{k\Delta x} s^2\gamma_\delta(s)ds \\ &\leq \left(1 - \frac{2\Delta t}{\Delta x^2}\sum_{k=1}^{r}\frac{1}{k^2}\int_{(k-1)\Delta x}^{k\Delta x} s^2\gamma_\delta(s)ds\right)M + \frac{\Delta t}{\Delta x^2}\sum_{k=1}^{r}\frac{M + M}{k^2}\int_{(k-1)\Delta x}^{k\Delta x} s^2\gamma_\delta(s)ds \\ &= M. \end{aligned} \tag{5.44}$$

Case II Transitional: Consider $i \in \{N + 1, ..., N + r\}$ which is the transitional region.

Then

$$
\begin{aligned}
u_i^{m+1} &\le u_i^m + \Delta t \mathcal{L}_{\delta,\Delta x}^{qnl} u_i^m \\
&= u_i^m + \Delta t \Bigg[\sum_{k=\frac{x_i}{\Delta x}+1}^{r} \frac{u_{i+k-1}^m - 2u_i^m + u_{i-k+1}^m}{2(k-1)^2 \Delta x^2} \int_{(k-1)\Delta x}^{k\Delta x} s^2 \gamma_\delta(s) ds \\
&- \sum_{k=\frac{x_i}{\Delta x}+1}^{r} \frac{u_{i+k-1}^m - u_{i-k+1}^m}{2(k-1)\Delta x} \int_{(k-1)\Delta x}^{k\Delta x} s\gamma_\delta(s) ds + \left(\int_{x_i}^{\delta} s\gamma_\delta(s) ds \right) \frac{u_{i+1}^m - u_i^m}{\Delta x} \\
&+ \left(\int_0^{x_i} s^2 \gamma_\delta(s) ds + x_i \int_{x_i}^{\delta} s\gamma_\delta(s) ds \right) \frac{u_{i+1}^m - 2u_i^m + u_{i-1}^m}{\Delta x^2} \Bigg] \\
&= A \cdot u_i^m + \sum_{k=\frac{x_i}{\Delta x}+1}^{r} \left(B_k \cdot u_{i+k-1}^m + C_k \cdot u_{i-k+1}^m + D \cdot u_{i+1}^m + E \cdot u_{i-1}^m \right)
\end{aligned} \tag{5.45}
$$

where those notations are defined as

$$
\begin{aligned}
A &= 1 + \frac{\Delta t}{\Delta x^2} \left(\sum_{k=\frac{x_i}{\Delta x}+1}^{r} \frac{-1}{(k-1)^2} \int_{(k-1)\Delta x}^{k\Delta x} s^2 \gamma_\delta(s) ds \right) + \frac{\Delta t}{\Delta x} \left(- \int_{x_i}^{\delta} s\gamma_\delta(s) ds \right) \\
&\quad - \frac{2\Delta t}{\Delta x^2} \left(\int_0^{x_i} s^2 \gamma_\delta(s) ds + x_i \int_{x_i}^{\delta} s\gamma_\delta(s) ds \right), \\
B_k &= \frac{\Delta t}{2\Delta x^2 (k-1)^2} \int_{(k-1)\Delta x}^{k\Delta x} s^2 \gamma_\delta(s) ds - \frac{\Delta t}{2\Delta x (k-1)} \int_{(k-1)\Delta x}^{k\Delta x} s\gamma_\delta(s) ds, \\
C_k &= \frac{\Delta t}{2\Delta x^2 (k-1)^2} \int_{(k-1)\Delta x}^{k\Delta x} s^2 \gamma_\delta(s) ds + \frac{\Delta t}{2\Delta x (k-1)} \int_{(k-1)\Delta x}^{k\Delta x} s\gamma_\delta(s) ds, \\
D &= \frac{\Delta t}{\Delta x} \int_{x_i}^{\delta} s\gamma_\delta(s) ds + \frac{\Delta t}{\Delta x^2} \left(\int_0^{x_i} s^2 \gamma_\delta(s) ds + x_i \int_{x_i}^{\delta} s\gamma_\delta(s) ds \right), \text{and} \\
E &= \frac{\Delta t}{\Delta x^2} \left(\int_0^{x_i} s^2 \gamma_\delta(s) ds + x_i \int_{x_i}^{\delta} s\gamma_\delta(s) ds \right).
\end{aligned} \tag{5.46}
$$

Clearly, $A + \sum_{k=\frac{x_i}{\Delta x}+1}^{r} (B_k + C_k) + D + E = 1$, and $B_k, C_k, D, E \ge 0$ when Δx is sufficiently small and because $-\frac{\Delta t}{2\Delta x(k-1)} \int_{(k-1)\Delta x}^{k\Delta x} s\gamma_\delta(s) ds > -\frac{\Delta t}{2(\Delta x)^2 (k-1)^2} \int_{(k-1)\Delta x}^{k\Delta x} s^2 \gamma_\delta(s) ds$.

Now we want to prove that $A \geq 0$. It is equivalent to prove

$$1 - A = \frac{\Delta t}{\Delta x^2}\Bigg[\sum_{k=\frac{x_i}{\Delta x}+1}^{r} \frac{1}{(k-1)^2}\int_{(k-1)\Delta x}^{k\Delta x} s^2\gamma_\delta(s)ds + 2\Bigg(\int_0^{x_i} s^2\gamma_\delta(s)ds + x_i\int_{x_i}^{\delta} s\gamma_\delta(s)ds\Bigg) + \Delta x\int_{x_i}^{\delta} s\gamma_\delta(s)ds\Bigg] \leq 1. \tag{5.47}$$

Notice that

$$\begin{aligned}
1 - A &= \frac{\Delta t}{\Delta x^2}\Bigg[\sum_{k=\frac{x_i}{\Delta x}+1}^{r}\Bigg(\frac{1}{(k-1)^2}\int_{(k-1)\Delta x}^{k\Delta x} s^2\gamma_\delta(s)ds + 2x_i\int_{(k-1)\Delta x}^{k\Delta x}\left(\frac{1}{s}\right)s^2\gamma_\delta(s)ds \\
&\quad + \Delta x\int_{(k-1)\Delta x}^{k\Delta x}\left(\frac{1}{s}\right)s^2\gamma_\delta(s)ds\Bigg) + 2\int_0^{x_i} s^2\gamma_\delta(s)ds\Bigg] \\
&\leq \frac{\Delta t}{\Delta x^2}\Bigg[\sum_{k=\frac{x_i}{\Delta x}+1}^{r}\Bigg(\frac{1}{(k-1)^2}\int_{(k-1)\Delta x}^{k\Delta x} s^2\gamma_\delta(s)ds + \frac{2x_i}{(k-1)\Delta x}\int_{(k-1)\Delta x}^{k\Delta x} s^2\gamma_\delta(s)ds \\
&\quad + \frac{\Delta x}{(k-1)\Delta x}\int_{(k-1)\Delta x}^{k\Delta x} s^2\gamma_\delta(s)ds\Bigg) + 2\int_0^{x_i} s^2\gamma_\delta(s)ds\Bigg] \\
&\leq \frac{\Delta t}{\Delta x^2}\Bigg[\sum_{k=\frac{x_i}{\Delta x}+1}^{r} 4\int_{(k-1)\Delta x}^{k\Delta x} s^2\gamma_\delta(s)ds + 4\int_0^{x_i} s^2\gamma_\delta(s)ds\Bigg] \\
&= 4\frac{\Delta t}{\Delta x^2}\Bigg[\sum_{k=\frac{x_i}{\Delta x}+1}^{r}\int_{(k-1)\Delta x}^{k\Delta x} s^2\gamma_\delta(s)ds + \int_0^{x_i} s^2\gamma_\delta(s)ds\Bigg] = \frac{4\Delta t}{\Delta x^2}\int_0^{\delta} s^2\gamma_\delta(s)ds \\
&= 4\frac{\Delta t}{\Delta x^2} \leq 1.
\end{aligned}$$

Since $\frac{\Delta t}{\Delta x^2} \leq \frac{1}{4}$, so $1 - A \leq 1$. Therefore,

$$A \geq 0 \text{ for } B_k \geq \frac{\Delta t}{2\Delta x^2(k-1)^2}\int_{(k-1)\Delta x}^{k\Delta x} s^2\gamma_\delta(s)ds - \frac{\Delta t}{2\Delta x^2(k-1)^2}\int_{(k-1)\Delta x}^{k\Delta x} s^2\gamma_\delta(s)ds = 0.$$

Summarizing the coefficients of equation (5.45) gives

- $A, B_k, C_k, D, E \geq 0$
- $A + \sum_{k=\frac{x_i}{\Delta x}+1}^{r}(B_k + C_k) + D + E = 1.$

Hence $u_i^{m+1} \leq \left(A + \sum_{k=\frac{x_i}{\Delta x}+1}^{r} (B_k + C_k) + D + E \right) M = M.$

Case III Local: Consider $i \in \{N + r + 1, ..., 2N - 1\}$ which is the local region. Then

$$u_i^{m+1} = u_i^m + \frac{\Delta t}{\Delta x^2}\left(u_{i+1}^m - 2u_i^m + u_{i-1}^m \right) + \Delta t f_i^m \leq \left(1 - \frac{2\Delta t}{\Delta x^2} \right) u_i^m + \frac{\Delta t}{\Delta x^2}\left(u_{i+1}^m + u_{i-1}^m \right)$$

with $\frac{\Delta t}{\Delta x^2} \leq \frac{1}{4}$ which gives all positive coefficients, so $u_i^{m+1} \leq M$.

Combining case I, II, III we can conclude that given $u_i^m \leq M$ for all $i \in I_\Omega$, and $\frac{\Delta t}{\Delta x^2} \leq \frac{1}{4}$ we have $u_i^{m+1} \leq M$ for all $i \in I_\Omega$. According to induction, the theorem is proved.

□

Corollary 2. *Suppose for $i \in I = I_\Omega \cup I_B$, $n = 0, 1, ..., N_T - 1$, and $T = N_T \cdot \Delta t$ that $\{u_i^n\}$ solves the following discrete QNL diffusion equation* (5.40) *then we have the following upper bound for u_i^n given that $\frac{\Delta t}{\Delta x^2} \leq \frac{1}{4}$,*

$$u_i^n \leq T \cdot ||f||_{\ell^\infty(I)} + max\{||g_i^0||_{\ell^\infty(I)}, ||q_i^n||_{\ell^\infty(I_B)}\}. \tag{5.48}$$

Proof. We introduce a comparison function

$$w_i^n = u_i^n + (T - n \cdot \Delta t)||f||_{\ell^\infty(I)} \geq u_i^n \tag{5.49}$$

for $i \in I$, and $n \geq 0$. Then we have

$$\frac{w_i^{n+1} - w_i^n}{\Delta t} = \frac{u_i^{n+1} - u_i^n}{\Delta t} - ||f||_{\ell^\infty(I)} = \mathcal{L}_{\delta,\Delta x}^{qnl} u_i^n + \left(f_i^n - ||f||_{\ell^\infty(I)} \right)$$

where $\left(f_i^n - ||f||_{\ell^\infty(I)} \right) \leq 0$. Therefore by Theorem 13, w_i^n satisfies the discrete maximum principle $w_i^n \leq \max\{w_i^0|_{i\in I},\ w_i^n|_{i\in I_B}\}$ for all $i \in I_\Omega$ and $n \geq 0$, given that $\frac{\Delta t}{\Delta x^2} \leq \frac{1}{4}$.

Notice that

$$w_i^0 = u_i^0 + T \cdot ||f||_{\ell^\infty(I)} \leq \max\{||g_i^0||_{\ell^\infty(I)}, ||q_i^n||_{\ell^\infty(I_B)}\} + T \cdot ||f||_{\ell^\infty(I)} \tag{5.50}$$

and also that

$$w_i^n|_{i\in I_B} = u_i^n|_{i\in I_B} + \Big(T - n\cdot\Delta t\Big)||f||_{\ell^\infty(I)} \leq \max\{||g_i^0||_{\ell^\infty(I)}, ||q_i^n||_{\ell^\infty(I_B)}\} + T\cdot||f||_{\ell^\infty(I)}. \tag{5.51}$$

combined with the fact that $u_i^n|_{i\in I} \leq w_i^n|_{i\in I}$ proves the corollary. □

Remark 3. *Although in the proof of the stability analysis, we require that* $\frac{\Delta t}{\Delta x^2} \leq \frac{1}{4}$ *to proceed with the analysis; meanwhile, we notice in the simulation that with* $\frac{\Delta t}{\Delta x^2}$ *close to* $\frac{1}{2}$*, we still have stable numerical results.*

5.4 Convergence of Discretized Quasi-nonlocal Operator

In this section, we prove the convergence results of the proposed FDM scheme.

Theorem 14. ***Global error estimate of the discrete solution*** *Suppose* $u(x,t)$ *is the strong solution to* (5.4) *and* u_i^n *is the discrete solution to the scheme* (5.7) *with* $i \in I, n = 0, 1, ..., N_T - 1$*, and* $N_T\Delta t = T$*, respectively. Then we have*

$$|u(x_i, t^n) - u_i^n| \leq T \cdot C_\delta(\Delta x + \Delta t) \tag{5.52}$$

given that $\frac{\Delta t}{\Delta x^2} \leq \frac{1}{4}$.

Proof. We define $e_i^n = u(x_i, t^n) - u_i^n$, $i = 1, 2, ..., 2N - 1$, $n = 0, 1, ..., N_T$ to be the error between the exact and discrete solutions. Then from the consistency analysis, and since $f_i^n = f(x_i, t^n)$, we have that

$$\begin{cases} \frac{e_i^{n+1}-e_i^n}{\Delta t} - \mathcal{L}_{\delta,\Delta x}^{qnl} e_i^n = \varepsilon_{c,i}, \quad for\ i \in I_\Omega,\ and\ n \geq 0 \\ e_i^0 = 0, i \in I \quad \text{(Initial Error)} \\ e_i^n = 0, \quad i \in I_B \quad \text{(Boundary Error)} \end{cases} \tag{5.53}$$

where $|\varepsilon_{c,i}| < C_\delta(\Delta x^2 + \Delta t)$ according to the consistency analysis. Hence we consider the following auxiliary function

$$w_i^n = e_i^n - (n\Delta t) \cdot C_\delta(\Delta x^2 + \Delta t). \tag{5.54}$$

Observe that

$$\begin{aligned} &\frac{w_i^{n+1} - w_i^n}{\Delta t} - \mathcal{L}_{\delta,\Delta x}^{qnl} w_i^n \\ &\quad = \frac{[e_i^{n+1} - C_\delta(\Delta x^2 + \Delta t)((n+1)\Delta t)] - [e_i^n - C_\delta(\Delta x^2 + \Delta t)(n\Delta t)]}{\Delta t} - \mathcal{L}_{\delta,\Delta x}^{qnl} e_i^n \\ &\quad = \frac{e_i^{n+1} - e_i^n}{\Delta t} - C_\delta(\Delta x^2 + \Delta t) - \mathcal{L}_{\delta,\Delta x}^{qnl} e_i^n \\ &\quad = \varepsilon_{c,i} - C_\delta(\Delta x + \Delta t) \leq 0. \end{aligned} \tag{5.55}$$

Then w_i^n satisfies

$$\begin{cases} \frac{w_i^{n+1}-w_i^n}{\Delta t} - \mathcal{L}_{\delta,\Delta x}^{qnl} w_i^n \leq 0, \quad i \in I_\Omega, \\ w_i^0 = 0, \quad i \in I, \quad \text{(Initial)}, \\ w_i^n = -(n\Delta t) \cdot C_\delta(\Delta x + \Delta t), \quad i \in I_B \quad \text{(Boundary)}, \end{cases} \tag{5.56}$$

because of the the discrete maximum principle proved in Theorem 13, so

$$w_i^n \leq \max\{w_i^0 | i \in I, \quad w_i^n|_{i \in I_B}\} = 0, \quad \forall i \in I_\Omega. \tag{5.57}$$

Therefore, $e_i^n \leq (n\Delta t) \cdot C_\delta(\Delta x + \Delta t)$. Similarly when $w_i^n = e_i^n + (n\Delta t) \cdot C_\delta(\Delta x + \Delta t)$

we have $e_i^n \geq -(n\Delta t)\cdot C_\delta(\Delta x+\Delta t)$. Hence, $|e_i^n| \leq (n\Delta t)\cdot C_\delta(\Delta x+\Delta t)$ which gives $|u(x_i,t^n)-u_i^n| \leq T\cdot C_\delta(\Delta x+\Delta t)$.

□

5.5 Study of the Courant-Friedricks-Lewy (CFL) Condiditon

In this section, we study the CFL condition of the new finite difference scheme by employing the Von Neumann stability analysis. We denote $\frac{\Delta t}{\Delta x}$ by λ_1 and $\frac{\Delta t}{(\Delta x)^2}$ by λ_2 and insert $u_i^n = (g(\theta))^n\, e^{\sqrt{-1}\theta x_i}$ into the scheme (5.6) where θ is a given wave number. We have the following three cases:

- **Case I Nonlocal**: for $x_i \leq 0$, the growth factor is

$$g(\theta) = 1+\lambda_2\sum_{j=1}^{r}\frac{2\big(\cos(\theta j\Delta x)-1\big)}{j^2}\int_{(j-1)\Delta x}^{j\Delta x} s^2\gamma_\delta(s)ds. \tag{5.58}$$

- **Case II Transitional**: for $0 < x_i \leq \delta$, the growth factor is

$$\begin{aligned} g(\theta) =& 1+\lambda_1\sum_{j=\frac{x_i}{\Delta x}+1}^{r}\frac{\big(\cos(\theta(j-1)\Delta x)-1\big)}{(j-1)}\int_{(j-1)\Delta x}^{j\Delta x} s\gamma_\delta(s)ds \\ &-\lambda_1\sum_{j=\frac{x_i}{\Delta x}+1}^{r}\frac{\sqrt{-1}\sin(\theta(j-1)\Delta x)}{(j-1)}\int_{(j-1)\Delta x}^{j\Delta x} s\gamma_\delta(s)ds \\ &+\lambda_1\left(\int_{x_i}^{\delta} s\gamma_\delta(s)ds\right)\big(\cos(\theta\Delta x)+\sqrt{-1}\sin(\theta\Delta x)-1\big) \\ &+\lambda_2\left(\int_0^{x_i} s^2\gamma_\delta(s)ds + x_i\int_{x_i}^{\delta} s\gamma_\delta(s)ds\right)\big(2\cos(\theta\Delta x)-2\big). \end{aligned} \tag{5.59}$$

- **Case III Local**: for $x_i > \delta$, the growth factor is

$$g(\theta) = 1+\lambda_2\big(2\cos(\theta\Delta x)-2\big). \tag{5.60}$$

Proof. Performing the Von Nuemman analysis for stability we substitute $u_i^n = (g(\theta))^n\, e^{\sqrt{-1}\theta x_i}$

Case I:

$$\frac{u_i^{n+1}-u_i^n}{\Delta t}=\sum_{j=1}^{r}\frac{u_{i+j}^n-2u_i^n+u_{i-j}^n}{(j\Delta x)^2}\int_{(j-1)\Delta x}^{j\Delta x}s^2\gamma_\delta(s)ds \tag{5.61}$$

Substituting $u_i^n=(g(\theta))^n\,e^{\sqrt{-1}\theta x_i}$ gives

$$g(\theta)^n e^{\sqrt{-1}\theta x_i}(g(\theta)-1)=\lambda_2\sum_{j=1}^{r}\frac{g(\theta)^n e^{\sqrt{-1}\theta x_i}\big(e^{\sqrt{-1}\theta\Delta x}-2+e^{-\sqrt{-1}\theta\Delta x}\big)}{j^2}\int_{(j-1)\Delta x}^{j\Delta x}s^2\gamma_\delta(s)ds. \tag{5.62}$$

Therefore, we can conclude the growth factor for the nonlocal region is

$$g(\theta)=1+\lambda_2\sum_{j=1}^{r}(\frac{2\big(\cos(\theta j\Delta x)-1\big)}{j^2}\int_{(j-1)\Delta x}^{j\Delta x}s^2\gamma_\delta(s)ds. \tag{5.63}$$

Case II:

$$\begin{aligned}\frac{u_i^{n+1}-u_i^n}{\Delta t}=&\sum_{j=\frac{x_i}{\Delta x}+1}^{r}\frac{u_{i+j-1}^n-2u_i^n+u_{i-j+1}^n}{2(j-1)\Delta x}\int_{(j-1)\Delta x}^{j\Delta x}s\gamma_\delta(s)ds\\&-\sum_{j=\frac{x_i}{\Delta x}+1}^{r}\frac{u_{i+j-1}^n-u_{i-j+1}^n}{2(j-1)\Delta x}\int_{(j-1)\Delta x}^{j\Delta x}s\gamma_\delta(s)ds\\&+\left(\int_{x_i}^{\delta}s\gamma_\delta(s)ds\right)\frac{u_{i+1}^n-u_i^n}{\Delta x}\\&+\left(\int_0^{x_i}s^2\gamma_\delta(s)ds+x_i\int_{x_i}^{\delta}s\gamma_\delta(s)ds\right)\frac{u_{i+1}^n-2u_i^n+u_{i-1}}{(\Delta x)^2}.\end{aligned} \tag{5.64}$$

Similarly to the nonlocal region substituting $u_i^n = (g(\theta))^n e^{\sqrt{-1}\theta x_i}$ gives

$$
\begin{aligned}
&g(\theta)^n e^{\sqrt{-1}\theta x_i}(g(\theta)-1) = \\
&\quad \lambda_1 \sum_{j=\frac{x_i}{\Delta x}+1}^{r} \frac{1}{2(j-1)} \Big(g(\theta)^n e^{\sqrt{-1}\theta x_i} \big(e^{\sqrt{-1}\theta(j-1)\Delta x} - 2 + e^{-\sqrt{-1}\theta(j-1)\Delta x} \big) \Big) \int_{(j-1)\Delta x}^{j\Delta x} s\gamma_\delta(s) ds \\
&\quad - \lambda_1 \sum_{j=\frac{x_i}{\Delta x}+1}^{r} \frac{1}{2(j-1)} \Big(g(\theta)^n e^{\sqrt{-1}\theta x_i} \big(e^{\sqrt{-1}\theta(j-1)\Delta x} - e^{-\sqrt{-1}\theta(j-1)\Delta x} \big) \Big) \int_{(j-1)\Delta x}^{j\Delta x} s\gamma_\delta(s) ds \\
&\quad + \lambda_1 \Big(\int_{x_i}^{\delta} s\gamma_\delta(s) ds \Big) \Big(g(\theta)^n e^{\sqrt{-1}\theta x_i} \big(e^{\sqrt{-1}k\Delta x} - 1 \big) \Big) \\
&\quad + \lambda_2 \Big(\int_0^{x_i} s^2 \gamma_\delta(s) ds + x_i \int_{x_i}^{\delta} s\gamma_\delta(s) ds \Big) \Big(g(\theta)^n e^{\sqrt{-1}\theta x_i} \big(e^{\sqrt{-1}\theta\Delta x} - 2 + e^{-\sqrt{-1}\theta\Delta x} \big) \Big).
\end{aligned}
\tag{5.65}
$$

Therefore, we can conclude the growth factor for the transitional region is

$$
\begin{aligned}
g(\theta) =& 1 + \lambda_1 \sum_{j=\frac{x_i}{\Delta x}+1}^{r} \frac{\big(\cos(\theta(j-1)\Delta x) - 1 \big)}{(j-1)} \int_{(j-1)\Delta x}^{j\Delta x} s\gamma_\delta(s) ds \\
&- \lambda_1 \sum_{j=\frac{x_i}{\Delta x}+1}^{r} \frac{\sqrt{-1}\sin(\theta(j-1)\Delta x)}{(j-1)} \int_{(j-1)\Delta x}^{j\Delta x} s\gamma_\delta(s) ds \\
&+ \lambda_1 \Big(\int_{x_i}^{\delta} s\gamma_\delta(s) ds \Big) \big(\cos(\theta\Delta x) + \sqrt{-1}\sin(k\Delta x) - 1 \big) \\
&+ \lambda_2 \Big(\int_0^{x_i} s^2 \gamma_\delta(s) ds + x_i \int_{x_i}^{\delta} s\gamma_\delta(s) ds \Big) \big(2\cos(\theta\Delta x) - 2 \big).
\end{aligned}
\tag{5.66}
$$

Case III:

$$
\frac{u_i^{n+1} - u_i^n}{\Delta t} = \frac{u_{i+1}^n - 2u_i^n + u_{i-1}^n}{(\Delta x)^2} \tag{5.67}
$$

Finally, substituting $u_i^n = (g(\theta))^n e^{\sqrt{-1}\theta x_i}$ gives

$$
g(\theta)^n e^{\sqrt{-1}\theta x_i}(g(\theta)-1) = \lambda_2 \Big(g(\theta)^n e^{\sqrt{-1}\theta x_i} \big(e^{\sqrt{-1}\theta\Delta x} - 2 + e^{-\sqrt{-1}k\Delta x} \big) \Big). \tag{5.68}
$$

Therefore, we can conclude the growth factor for the local region is

$$g(\theta) = 1 + \lambda_2\big(2\cos(\theta\Delta x) - 2\big). \tag{5.69}$$

Clearly, we have $\lambda_2 = \Delta x\lambda_1$, so once we get the CFL constraint on λ_1, the CFL condition for λ_2 will be satisfied when Δx is sufficiently small. Because it is very difficult to analytically find this upper bound we implement the growth factor $g(\theta)$ numerically to identify restrictions on λ_1 and λ_2 to ensure $|g(\theta)| \leq 1$. □

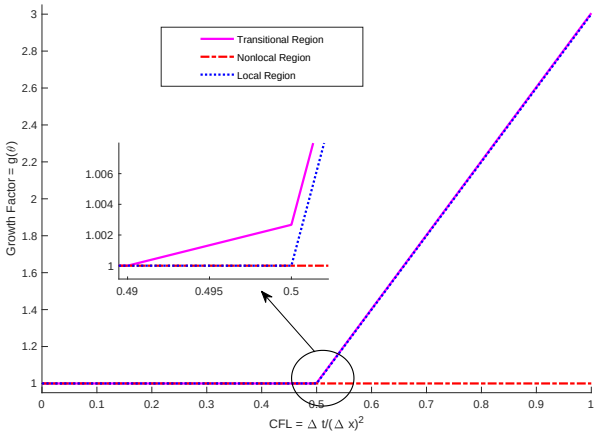

Figure 5.3: Maximum Growth Rate of (5.58), (5.59), (5.60) for the new finite difference method versus that of (5.8) for the original finite difference method.

For linear local diffusion models with explicit Euler integration and the middle-point finite-difference discretization, the CFL is restricted by CFL $= \frac{\Delta t}{\Delta x^2} \leq 0.5$. This provides the largest step size in time to reduce computational cost while preserves stability. By numerically analyzing the growth factor in Figure 5.3, we found that the nonlocal and local regions match the typical restrictions for stability, but the transitional region is slightly less than 0.5. This factor needs to be considered for stability restrictions to the CFL on the whole coupling system. On the other hand, compared with the original FDM scheme proposed in [14], the new FDM discretization can afford a larger CFL condition, which suggests that the new scheme is more stable.

5.6 Numerical Examples

In this section, we test several numerical examples to confirm the stability and convergence results. We fix the nonlocal diffusion kernel to be a constant kernel

$$\gamma_\delta(s) = \frac{3}{\delta^3}\chi_{[-\delta,\,\delta]}(s).$$

1. For the first example, we consider the asymptotic compatibility (AC) of the discretized operator $\mathcal{L}^{qnl}_{\delta,\Delta x}$ to the local diffusion problem as the horizon δ and spatial discretization Δx go to zero at the same time.

   We consider the external force f as

   $$f(x,t) = 30x^4e^{-t} + e^{-t}(x^6-1) + 2. \tag{5.70}$$

   Then, the exact solution to the local diffusion ${u^\ell}_t = u^\ell_{xx} + f$ with $u^\ell(-1,t) = u^\ell(1,t) = 0$ and $u^\ell(x,0) = (1-x^2) - (x^6-1)$ is

   $$u^\ell(x,t) = (1-x^2) - e^{-t}(x^6-1). \tag{5.71}$$

   To test the AC convergence, we fix $\delta = r\Delta$ with $r = 3$ and set the CFL to be $CFL = 0.45$, that is $\Delta t = 0.2\Delta x$, and the termination time is chosen to be $T = 1$.

   First order convergence with respect to Δx is observed. The convergence order and $L^\infty_{\Omega\times[0,T]}$ differences between $u^\ell(x,t)$ and discrete solution of $u^{qnl}_{\delta,\Delta x}$ are listed in Table 5.1. Also the visual comparison of the two solutions at $t = 0$ and $t = T$ are displayed in Figure 5.4 with good agreement.

Table 5.1: $L^{\infty}_{\Omega\times[0,T]}$ differences between the local continuous solution u^{ℓ} and discrete solution $u^{qnl}_{\delta,\Delta x}$. We fix $\delta = 3\Delta x$, and the kernel is $\gamma_{\delta}(s) = \frac{3}{\delta^3}\chi_{[-\delta,\delta]}(s)$. The termination time $T = 1$ and $\Delta t = 0.2\Delta x$.

Δx	$\|\|u^{\ell}(x_i,t^n) - u^{qnl}_{\delta,\Delta x}(x_i,t^n)\|\|_{L^{\infty}_{\Omega\times[0,T]}}$	Order
$\frac{1}{50}$	0.1422	–
$\frac{1}{100}$	7.168e−2	0.988
$\frac{1}{200}$	3.614e−2	0.988
$\frac{1}{400}$	1.820e−2	0.990
$\frac{1}{800}$	9.151e−3	0.992
$\frac{1}{1600}$	4.594e−3	0.994

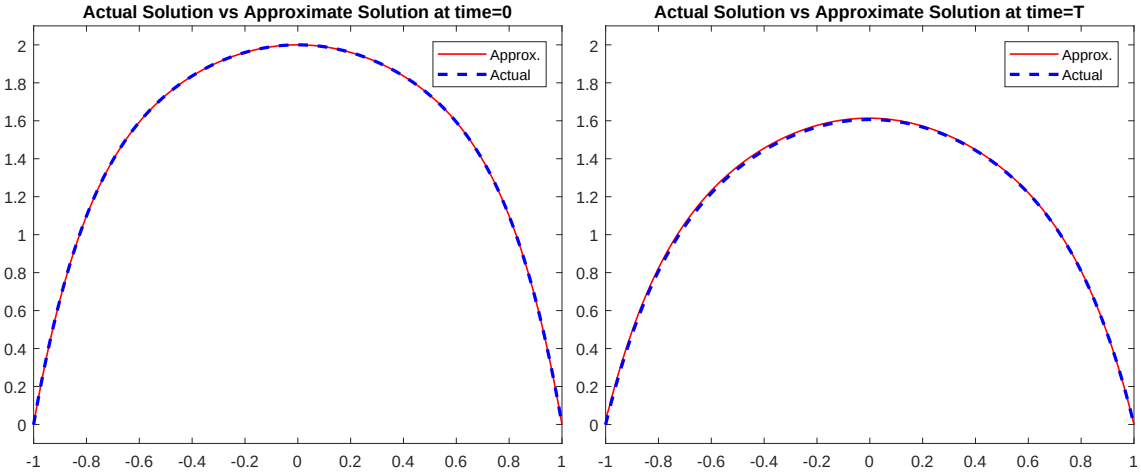

(a) solutions at $t = 0$

(b) solutions at $t = 1$

Figure 5.4: Plots of solutions to the approximate and actual solutions. The kernel function was chosen as $\gamma_{\delta}(s) = \frac{3}{\delta^3}\chi_{[-\delta,\delta]}(s)$. The coupling inference is at $x^* = 0$, and the mesh size is $\Delta x = \frac{1}{400}$ with a horizon as $\delta = \frac{3}{400}$, the temporal step size is $\Delta t = 0.45\Delta x$.

2. In the following example, we compare the original scheme $\tilde{\mathcal{L}}^{qnl}_{\delta}$ (5.8) proposed in [14] with the new proposed scheme $\mathcal{L}^{qnl}_{\delta,\Delta x}$ in (5.6).

   We are going to compare the AC convergence between (5.6) and (5.8). The exact local

continuous solution is chosen to be

$$u^{\ell}(x,t) = e^{-t}(1-x)^2(1+x)^2x^2 \tag{5.72}$$

and the corresponding external force is

$$\begin{aligned} f(x,t) =& u_t^{\ell} - u_{xx}^{\ell} \\ =& - e^{-t}\left((x-x^3)^2 + (2-24x^2+30x^4)\right). \end{aligned} \tag{5.73}$$

Again the kernel used is $\gamma_\delta(s) = \frac{3}{\delta^3}$ with $\delta = 3\Delta x$. We denote the solution obtained by $\mathcal{L}^{qnl}_{\delta,\Delta x}$ by $u^{qnl}_{\delta,\Delta x}$ and the solution obtained by $\tilde{\mathcal{L}}^{qnl}_{\delta,\Delta x}$ by $\tilde{u}^{qnl}_{\delta,\Delta x}$.

First order AC convergence with respect to Δx are observed in Table 5.2 for both schemes (5.6) and (5.8), respectively. The approximation using scheme (5.6) at larger step size has a second order convergence rate, and at smaller step size tends to be of first order.

Table 5.2: $L^{\infty}_{\Omega\times[0,T]}$ differences between the local continuous solution u^{ℓ} and two discrete solutions $u^{qnl}_{\delta,\Delta x}$, $\tilde{u}^{qnl}_{\delta,\Delta x}$ using the FDM schemes (5.6) and (5.8), respectively. We fix $\delta = 3\Delta x$, and the kernel is $\gamma_\delta(s) = \frac{3}{\delta^3}$. The termination time is $T = 1$ and $\Delta t = 0.2\Delta x$.

Δx	$\|\|u^{\ell}(x_i,t^n) - \tilde{u}^{qnl}_{\delta,\Delta x}(x_i,t^n)\|\|_{L^\infty}$	Order	$\|\|u^{\ell}(x_i,t^n) - u^{qnl}_{\delta,\Delta x}(x_i,t^n)\|\|_{L^\infty}$	Order
$\frac{1}{50}$	9.255e−3	–	7.200e−3	–
$\frac{1}{100}$	4.692e−3	0.980	1.698e−3	2.08
$\frac{1}{200}$	2.356e−3	0.994	4.121e−4	1.09
$\frac{1}{400}$	1.179e−3	0.998	1.931e−4	1.09
$\frac{1}{800}$	5.900e−4	0.999	9.628e−5	1.00
$\frac{1}{1600}$	2.951e−4	1.00	4.806e−5	1.00

Next, we compare the three solutions obtained from the new scheme (1), the exact local continuous solution (2), and the original scheme (3) in Figure 5.5. Notice that the exact local continuous solution $u^{\ell}(x,t)$ should remain non negative throughout the entire computational domain $\Omega\times[0,T]$, however, both $u^{qnl}_{\delta,\Delta x}$ and $\tilde{u}^{qnl}_{\delta,\Delta x}$ become slightly negative around the interface

$x^* = 0$. This does not contradict the discrete maximum principle of $\mathcal{L}^{qnl}_{\delta,\Delta x}$ as the external force $f(x,t)$ defined in (5.73) does not retain negativity on $[-1,1]$ as required in the assumption of Theorem 13.

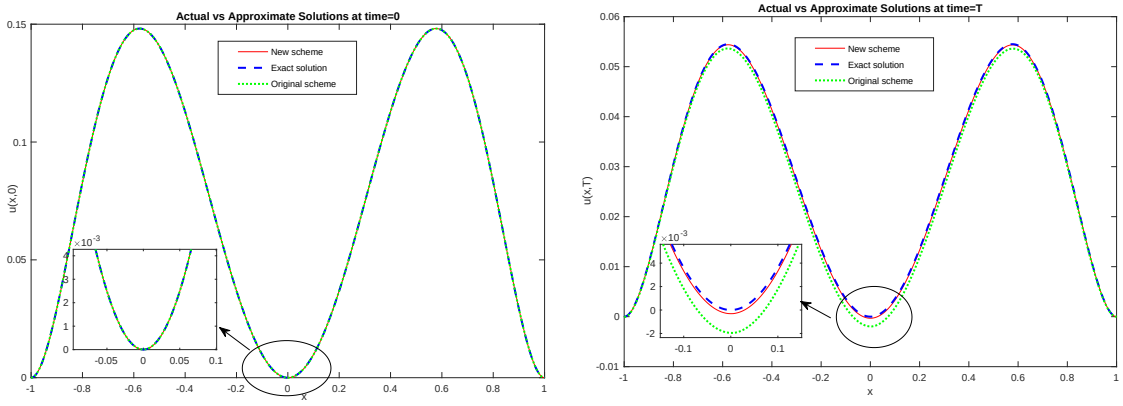

(a) solutions at $t = 0$ (b) solutions at $t = 1$

Figure 5.5: Numerical comparison between the new scheme (5.6) and original scheme (5.8) used to approximate (5.72) with external force given by (5.73). The spatial step size is $\Delta x = \frac{1}{200}$ and Δt=$0.25\Delta x$.

5.7 New Finite Difference Scheme Conclusion

We propose a new scheme to discretize the quasi-nonlocal (QNL) coupling operator introduced in [14] for the nonlocal-to-local diffusion problem. This new finite difference approximation preserves the properties of continuous equation on a discrete level. Consistency, stability, the maximum principle and the global convergence analysis of the scheme are proved rigorously. We analytically find the CFL conditions through the Von Neumann stability analysis and numerically calculate the CFL values for a given spatial discretization. The numerical calculations of the CFL provide an additional alert around the interface when considering the temporal step size for an explicit time integrator. The CFL restrictions on the transitional region were discovered to be slightly less than $\frac{1}{2}$ with the explicit Euler method employed in a diffusion problem. Multiple numerical examples are then provided and summarized to verify the theoretical findings. A comparison with the original scheme used in [14] is also provided which confirmed the improvements of the new scheme.

CHAPTER 6: DEVELOPMENT OF COEFFICIENT MATRICIES AND ADDITION OF NEUMANN AND ROBIN BOUNDARY CONDITIONS

In this chapter we develop the coefficient matrices, and explore the affects of Neumann and Robin Boundary conditions on the approximate results produced by the nonlocal to local finite difference scheme of this dissertation. Recall the heat equation

$$u_t(x,t) = u_{xx}(x,t) + f(x,t), \tag{6.1}$$

and the heat equation with Nonlocal to Local Coupling Operator and Dirichlet Boundary Conditions

$$\begin{cases} u_t(x,t) = \mathcal{L}^{qnl}u(x,t) + f(x,t) & x \in [-1,1] \\ u(x,0) = u_0(x) & x \in (-1,1) \\ u(x,t) = 0 & x \in [-\delta - 1, -1] \cup \{1\} \end{cases} \tag{6.2}$$

It is also useful in the development of the Coefficient Matrix to recall the 1-Dimensional Quasi-nonlocal Energy

$$E^{qnl}(u) = \frac{1}{2} \iint\limits_{x \leq \cup y \leq 0} \gamma_\delta(|y-x|)(u(y)-u(x))^2 dydx + \frac{1}{2} \int\limits_{x<0} |u'(x)|^2 \omega_\delta(x) dx \tag{6.3}$$

with the weight function definition and characteristics

$$\omega_\delta(x) = \int\limits_0^1 dt \int\limits_{|s|<\frac{x}{t}} |s|^2 \gamma(|s|) ds \tag{6.4}$$

$$\omega_\delta(x) = 2\int_0^x s^2\gamma_\delta(|s|)ds + 2x\int_x^\infty s\gamma_\delta(|s|)ds \tag{6.5}$$

$$\omega'_\delta(x) = 2\int_x^\infty s\gamma_\delta(s)ds. \tag{6.6}$$

The kernel is defined as

$$\begin{cases} \gamma_\delta(|s|) = \dfrac{1}{\delta^3}\gamma\left(\dfrac{|s|}{\delta}\right), \quad \gamma \text{ is nonnegative and nonincreasing on (0,1),} \\ \text{with supp}(\gamma) \subset [0,1] \text{ and } \displaystyle\int_{-\delta}^{\delta} |s|^2\gamma(|s|)ds = 2\,. \end{cases} \tag{6.7}$$

In Chapter 4 the continuous LNL operator was derived based on energy variation, and is

$$\mathcal{L}^{qnl}u(x) = \begin{cases} 2\int\limits_{y\in R} \gamma_\delta(|y-x|)(u(y)-u(x))dy, \text{ if } x<0 \\ 2\int\limits_{y<0} \gamma_\delta(|y-x|)\Big(u(y)-u(x)\Big)dy + (\omega_\delta(x)u'(x))', \text{ if } x\in[0,\delta) \\ u''(x), \text{ if } x\geq\delta. \end{cases}$$

In the next section we will derive the numerical operator from the continuous operator, and develop the coefficient matrix for Dirichlet Boundary Conditions.

6.1 Derivation of the Numerical Operator from the Continuous Operator and development of Coefficient Matrix for Dirichlet Boundary Conditions

Theorem 15. *The following are the equivalencies of the Continuous and Numerical Operators*

Nonlocal Domain

$$\begin{aligned}\mathcal{L}_\delta^{qnl}u(x,t) &= \int_{-\delta}^{\delta}\Big(u(x+s,t)-u(x,t)\Big)\gamma_\delta(s)ds \\ &= \sum_{j=1}^{r}\frac{\gamma h(j^3-(j-1)^3)}{3j^2}u_{i+j}^n - \frac{2\gamma h(j^3-(j-1)^3)}{3j^2}u_i^n + \frac{\gamma h(j^3-(j-1)^3)}{3j^2}u_{i-j}^n\end{aligned} \tag{6.8}$$

Transitional Domain

$$\begin{aligned}\mathcal{L}_\delta^{qnl}u(x,t) &= \int_x^\delta \gamma_\delta(s)\Big(u(x-s,t)-u(x,t)\Big)ds + \left(\int_x^\delta s\gamma_\delta(s)ds\right)u_x(x,t) \\ &+ \left(\int_0^x s^2\gamma_\delta(s) + x\int_x^\delta s\gamma_\delta(s)ds\right)u_{xx}(x) \\ &= \sum_{j=\frac{x_i}{h}+1}^{r}(u_{i+j-1}^n - 2u_i^n + u_{i-j+1}^n)\left(\frac{\gamma h(j^2-(j-1)^2)}{4(j-1)}\right) \\ &- \sum_{j=\frac{x_i}{h}+1}^{r}(u_{i+j-1}^n - u_{i-j+1}^n)\left(\frac{\gamma h(j^2-(j-1)^2)}{4(j-1)}\right) \\ &+ \left(\frac{\gamma(\delta^2-x_i^2)}{2h}\right)(u_{i+1}^n - u_i^n) \\ &+ \left(\left(\frac{\gamma {x_i}^3}{3h^2}\right) + x_i\left(\frac{\gamma(\delta^2-x_i^2)}{2h^2}\right)\right)(u_{i+1}^n - 2u_i^n + u_{i-1}^n)\end{aligned} \tag{6.9}$$

Local Domain

$$\begin{aligned}u_{xx}(x,t) &= \frac{u(x_{i+1},t)-2u(x_i,t)+u(x_{i-1},t)}{h^2} \\ &= \frac{1}{h^2}u_{i-1}^n - \frac{2}{h^2}u_i^n + \frac{1}{h^2}u_{i+1}^n\end{aligned} \tag{6.10}$$

Proof. **Nonlocal Domain:** Symmetry of $u(x,t)$ gives the following rearrangement of the continuous operator

$$\begin{aligned}
\mathcal{L}_\delta^{qnl}u(x,t) &= \int_{-\delta}^{\delta}\Big(u(x+s,t)-u(x,t)\Big)\gamma_\delta(s)ds \\
&= 2\int_0^{\delta}\gamma_\delta(s)\Big(u(x+s,t)-u(x,t)\Big)\gamma_\delta(s)ds \\
&= \int_0^{\delta}\gamma_\delta(s)\Big(2u(x+s,t)-2u(x,t)\Big)\gamma_\delta(s)ds \\
&= \int_0^{\delta}\gamma_\delta(s)\Big(u(x+s,t)-2u(x,t)+u(x-s,t)\Big)\gamma_\delta(s)ds
\end{aligned} \tag{6.11}$$

Next we discretize the continuous model such that

$$\begin{aligned}
\mathcal{L}_\delta^{qnl}u(x,t) &= \sum_{j=1}^{r}\int_{(j-1)h}^{jh} s^2\gamma_\delta(s)\left(\frac{u(x+s,t)-2u(x,t)+u(x-s,t)}{s^2}\right)ds \\
&= \sum_{j=1}^{r}\frac{u(x_{i+j},t^n)-2u(x_i,t^n)+u(x_{i-j},t^n)}{(jh)^2}\int_{(j-1)h}^{jh} s^2\gamma_\delta(s)ds \\
&= \sum_{j=1}^{r}\frac{u_{i+j}^n-2u_i^n+u_{i-j}^n}{(jh)^2}\left(\frac{1}{3}s^3\gamma|_{(j-1)h}^{jh}\right) \\
&= \sum_{j=1}^{r}\frac{u_{i+j}^n-2u_i^n+u_{i-j}^n}{(jh)^2}\left(\frac{1}{3}h^3\gamma\Big(j^3-(j-1)^3\Big)\right) \\
&= \sum_{j=1}^{r}\frac{\gamma h(j^3-(j-1)^3)}{3j^2}u_{i+j}^n-\frac{2\gamma h(j^3-(j-1)^3)}{3j^2}u_i^n+\frac{\gamma h(j^3-(j-1)^3)}{3j^2}u_{i-j}^n
\end{aligned} \tag{6.12}$$

Transitional Domain: In an earlier proof

$$\begin{aligned}
\mathcal{L}_{\delta}^{qnl}u(x,t) &= \int_{x}^{\delta}\gamma_{\delta}(s)\Big(u(x-s,t)-u(x,t)\Big)ds+\bigg(\int_{x}^{\delta}s\gamma_{\delta}(s)ds\bigg)u_{x}(x,t)\\
&+\bigg(\int_{0}^{x}s^{2}\gamma_{\delta}(s)+x\int_{x}^{\delta}s\gamma_{\delta}(s)ds\bigg)u_{xx}(x)\\
&=\sum_{j=\frac{x_i}{h}+1}^{r}\frac{u_{i+j-1}^{n}-2u_{i}^{n}+u_{i-j+1}^{n}}{2(j-1)h}\int_{(j-1)h}^{jh}s\gamma_{\delta}(s)ds\\
&-\sum_{j=\frac{x_i}{h}+1}^{r}\frac{u_{i+j-1}^{n}-u_{i-j+1}^{n}}{2(j-1)h}\int_{(j-1)h}^{jh}s\gamma_{\delta}(s)ds\\
&+\bigg(\int_{x_i}^{\delta}s\gamma_{\delta}(s)ds\bigg)\frac{u_{i+1}^{n}-u_{i}^{n}}{h}\\
&+\bigg(\int_{0}^{x_i}s^{2}\gamma_{\delta}(s)ds+x_i\int_{x_i}^{\delta}s\gamma_{\delta}(s)ds\bigg)\frac{u_{i+1}^{n}-2u_{i}^{n}+u_{i-1}^{n}}{(h)^{2}}. \qquad (6.13)
\end{aligned}$$

Then the discretized continuous operator can be written as

$$\begin{aligned}
\mathcal{L}_{\delta}^{qnl}u(x,t) &=\sum_{j=\frac{x_i}{h}+1}^{r}\frac{u_{i+j-1}^{n}-2u_{i}^{n}+u_{i-j+1}^{n}}{2(j-1)h}\left(\frac{s^{2}\gamma}{2}\bigg|_{(j-1)h}^{jh}\right)\\
&-\sum_{j=\frac{x_i}{h}+1}^{r}\frac{u_{i+j-1}^{n}-u_{i-j+1}^{n}}{2(j-1)h}\left(\frac{s^{2}\gamma}{2}\bigg|_{(j-1)h}^{jh}\right)\\
&+\left(\frac{s^{2}\gamma}{2}\bigg|_{x_i}^{\delta}\right)\frac{u_{i+1}^{n}-u_{i}^{n}}{h}\\
&+\left(\left(\frac{s^{3}\gamma}{3}\bigg|_{0}^{x_i}\right)+x_i\left(\frac{s^{2}\gamma}{2}\bigg|_{x_i}^{\delta}\right)\right)\frac{u_{i+1}^{n}-2u_{i}^{n}+u_{i-1}^{n}}{(h)^{2}}\\
&=\sum_{j=\frac{x_i}{h}+1}^{r}(u_{i+j-1}^{n}-2u_{i}^{n}+u_{i-j+1}^{n})\left(\frac{\gamma h(j^{2}-(j-1)^{2})}{4(j-1)}\right)\\
&-\sum_{j=\frac{x_i}{h}+1}^{r}(u_{i+j-1}^{n}-u_{i-j+1}^{n})\left(\frac{\gamma h(j^{2}-(j-1)^{2})}{4(j-1)}\right)\\
&+\left(\frac{\gamma(\delta^{2}-x_i^{2})}{2h}\right)(u_{i+1}^{n}-u_{i}^{n})\\
&+\left(\left(\frac{\gamma {x_i}^{3}}{3h^{2}}\right)+x_i\left(\frac{\gamma(\delta^{2}-x_i^{2})}{2h^{2}}\right)\right)(u_{i+1}^{n}-2u_{i}^{n}+u_{i-1}^{n}) \qquad (6.14)
\end{aligned}$$

Note: $r = 3$ is the radius used in all testing, so there are only ever 3 nodes within the transition region no matter the domain and step size.

Local Domain: By Central Difference

$$\begin{aligned} u_{xx}(x,t) &= \frac{u(x_{i+1},t) - 2u(x_i,t) + u(x_{i-1},t)}{h^2} \\ &= \frac{1}{h^2}u_{i-1}^n - \frac{2}{h^2}u_i^n + \frac{1}{h^2}u_{i+1}^n \end{aligned} \tag{6.15}$$

□

It is established that $r = 3$. Then $\delta = rh = 3h$ and $\gamma = \frac{3}{\delta^3} = \frac{3}{r^3h^3}$. N is the spatial index that determines step size $h = \frac{1}{N}$ and there are total of $2N + r + 1$ nodes where 5 nodes are part of the boundaries and boundary radius, $N - 1$ nodes from the Nonlocal section, 3 nodes from the Transitional section, and $N - 3$ nodes for the local section on the domain $[-1 - \delta, 1]$, or any domain.

Example: Let $N = 5$ then $h = \frac{1}{5} = 0.2$, $\delta = 0.6$, and the domain is discretized as follows.

Boundary Regions: $\{x_1, x_2, x_3, x_4, x_{14}\} = \{-1.6, -1.4, -1.2, -1, 1\}$

Nonlocal Region: $\{x_5, x_6, x_7, x_8\} = \{-0.8, -0.6, -0.4, -0.2\}$

Transitional Region $\{x_9, x_{10}, x_{11}\} = \{0, 0.2, 0.4\}$

Local Region $\{x_{12}, x_{13}\} = \{0.6, 0.8\}$

$$\begin{bmatrix} 1 & 0 & 0 & 0 & 0 & 0 & 0 & 0 & 0 & 0 & 0 & 0 & 0 & 0 \\ 0 & 1 & 0 & 0 & 0 & 0 & 0 & 0 & 0 & 0 & 0 & 0 & 0 & 0 \\ 0 & 0 & 1 & 0 & 0 & 0 & 0 & 0 & 0 & 0 & 0 & 0 & 0 & 0 \\ 0 & 0 & 0 & 1 & 0 & 0 & 0 & 0 & 0 & 0 & 0 & 0 & 0 & 0 \\ 0 & 0 & 0 & 0 & NL & NL & NL & NL & 0 & 0 & 0 & 0 & 0 & 0 \\ 0 & 0 & 0 & 0 & NL & NL & NL & NL & NL & 0 & 0 & 0 & 0 & 0 \\ 0 & 0 & 0 & 0 & NL & NL & NL & NL & NL & NL & 0 & 0 & 0 & 0 \\ 0 & 0 & 0 & 0 & NL & NL & NL & NL & NL & NL & NL & 0 & 0 & 0 \\ 0 & 0 & 0 & 0 & 0 & 0 & T & T & T & T & T & 0 & 0 & 0 \\ 0 & 0 & 0 & 0 & 0 & 0 & 0 & T & T & T & T & T & 0 & 0 \\ 0 & 0 & 0 & 0 & 0 & 0 & 0 & 0 & T & T & T & T & T & 0 \\ 0 & 0 & 0 & 0 & 0 & 0 & 0 & 0 & 0 & 0 & L & L & L & 0 \\ 0 & 0 & 0 & 0 & 0 & 0 & 0 & 0 & 0 & 0 & 0 & L & L & 0 \\ 0 & 0 & 0 & 0 & 0 & 0 & 0 & 0 & 0 & 0 & 0 & 0 & 0 & 1 \end{bmatrix} \cdot \begin{bmatrix} u_1 \\ u_2 \\ u_3 \\ u_4 \\ u_5 \\ u_6 \\ u_7 \\ u_8 \\ u_9 \\ u_{10} \\ u_{11} \\ u_{12} \\ u_{13} \\ u_{14} \end{bmatrix} = \begin{bmatrix} f_1 \\ f_2 \\ f_3 \\ f_4 \\ f_5 \\ f_6 \\ f_7 \\ f_8 \\ f_9 \\ f_{10} \\ f_{11} \\ f_{12} \\ f_{13} \\ f_{14} \end{bmatrix}$$

Due to the boundary conditions $u(x,t) = 0$ for x in the boundary region the Stiffness/Coefficient Matrix can be reduced to

$$\begin{bmatrix} NL & NL & NL & NL & 0 & 0 & 0 & 0 & 0 \\ NL & NL & NL & NL & NL & 0 & 0 & 0 & 0 \\ NL & NL & NL & NL & NL & NL & 0 & 0 & 0 \\ NL & NL & NL & NL & NL & NL & NL & 0 & 0 \\ 0 & 0 & T & T & T & T & T & 0 & 0 \\ 0 & 0 & 0 & T & T & T & T & T & 0 \\ 0 & 0 & 0 & 0 & T & T & T & T & T \\ 0 & 0 & 0 & 0 & 0 & 0 & L & L & L \\ 0 & 0 & 0 & 0 & 0 & 0 & 0 & L & L \end{bmatrix} \cdot \begin{bmatrix} u_5 \\ u_6 \\ u_7 \\ u_8 \\ u_9 \\ u_{10} \\ u_{11} \\ u_{12} \\ u_{13} \end{bmatrix} = \begin{bmatrix} f_5 \\ f_6 \\ f_7 \\ f_8 \\ f_9 \\ f_{10} \\ f_{11} \\ f_{12} \\ f_{13} \end{bmatrix}$$

This is the general structure of the coefficient matrix for the previous numerical examples with Dirichlet Boundary Conditions.

Nonlocal Region Constants

$$\begin{aligned} \mathcal{L}^{\mathbf{NL}}u(x,t) &= \sum_{j=1}^{r} \frac{\gamma h(j^3-(j-1)^3)}{3j^2}u_{i+j}^n - \frac{2\gamma h(j^3-(j-1)^3)}{3j^2}u_i^n + \frac{\gamma h(j^3-(j-1)^3)}{3j^2}u_{i-j}^n \\ &= \sum_{j=1}^{r} \left(\frac{3j^2+3j+1}{r^3h^2j^2}\right)u_{i+j}^n + \left(\frac{-2(3j^2+3j+1)}{r^3h^2j^2}\right)u_i^n + \left(\frac{3j^2+3j+1}{r^3h^2j^2}\right)u_{i-j}^n \end{aligned}$$

$$\text{Therefore, } \left(\frac{3j^2+3j+1}{r^3h^2j^2}\right) \text{ Nonlocal Diffusion Constant } \mathbf{NL} \tag{6.16}$$

Transitional Region Constants

$$
\begin{aligned}
\mathcal{L}^{\mathbf{T}}u(x,t) = & \sum_{j=\frac{x_i}{h}+1}^{r}(u_{i+j-1}^n - 2u_i^n + u_{i-j+1}^n)\left(\frac{\gamma h(j^2-(j-1)^2)}{4(j-1)}\right) \\
& - \sum_{j=\frac{x_i}{h}+1}^{r}(u_{i+j-1}^n - u_{i-j+1}^n)\left(\frac{\gamma h(j^2-(j-1)^2)}{4(j-1)}\right) \\
& + \left(\frac{\gamma(\delta^2-x_i^2)}{2h}\right)(u_{i+1}^n - u_i^n) \\
& + \left(\left(\frac{\gamma {x_i}^3}{3h^2}\right) + x_i\left(\frac{\gamma(\delta^2-x_i^2)}{2h^2}\right)\right)(u_{i+1}^n - 2u_i^n + u_{i-1}^n) \\
& = \sum_{j=\frac{x_i}{h}+1}^{r}(u_{i+j-1}^n - 2u_i^n + u_{i-j+1}^n)\left(\frac{3(2j-1)}{4r^3h^2(j-1)}\right) \text{ Nonlocal Gradient Constant} \\
& - \sum_{j=\frac{x_i}{h}+1}^{r}(u_{i+j-1}^n - u_{i-j+1}^n)\left(\frac{3(2j-1)}{4r^3h^2(j-1)}\right) \text{ Nonlocal Gradient Constant} \\
& + \left(\frac{3}{2\delta h}\left(1-\left(\frac{x_i}{\delta}\right)^2\right)\right)(u_{i+1}^n - u_i^n) \text{ Local Gradient Constant} \\
& + \left(-\frac{1}{2}\left(\frac{x_i}{\delta}\right)^3 + \frac{3}{2}\left(\frac{x_i}{\delta}\right)\right)(u_{i+1}^n - 2u_i^n + u_{i-1}^n) \text{ Local Diffusion Constant} \quad (6.17)
\end{aligned}
$$

Local Region Constants

$$
\mathcal{L}^{\mathbf{L}} = \frac{1}{h^2}u_{i-1}^n - \frac{2}{h^2}u_i^n + \frac{1}{h^2}u_{i+1}^n \tag{6.18}
$$

$$
\text{Therefore, } \frac{1}{h^2} \text{ Local Diffusion Constant } \mathbf{L}
$$

In the published works [34], [47] studies were done with non-Dirichlet boundary conditions. To see the full picture of how the local to nonlocal finite difference scheme applies to diffusion problems, we also examined non-Dirichlet boundary conditions. The next two sections discuss the development of the coefficient matrix for the local to nonlocal diffusion finite difference scheme with Neumann and Robin boundary conditions. Recall Theorem 10, the

continuous local to nonlocal operator was derived based on energy variation. This definition of the continuous operator was transformed into the numerical operator used throughout this work. If you apply Neumann or Robin boundary conditions instead of Dirichlet in the development of the numerical operator you will see that the Neumann boundary conditions do not change the operator, but the Robin boundary conditions will.

6.2 Coefficient Matrix with Neumann Boundary Conditions and Numerical Example

Now we will consider the Neumann LNL boundary condition problem

$$\begin{cases} u_t(x,t) = \mathcal{L}^{qnl}u(x,t) + f(x,t) & x \in [-1,1] \\ u(x,0) = u_0(x) & x \in (-1,1) \\ u_x(x,t) = 0 & x \in [-\delta - 1, -1] \cup \{1\} \end{cases}$$

with the same conditions as described in the previous section.The Neumann boundary conditions and definition of $u_x(x,t)$ give

$$u_x(-1-3h,t) = u_x(-1-2h,t) = u_x(-1-h,t) = u_x(-1,t) = u_x(1,t) = 0 \tag{6.19}$$

which have nodal placement at

$$u_x(x_1,t) = u_x(x_2,t) = u_x(x_3,t) = u_x(x_4,t) = u_x(x_{2N+r+1},t) = 0, \tag{6.20}$$

and

$$u_x(x,t) = \frac{u(x+h,t) - u(x,t)}{h}. \tag{6.21}$$

Then

$$u_x(x_1,t) = \frac{u(x_2,t) - u(x_1,t)}{h} = 0 \tag{6.22}$$

which gives

$$-u_1 + u_2 = 0. \tag{6.23}$$

Similarly

$$\begin{aligned} -u_2 + u_3 &= 0 \\ -u_3 + u_4 &= 0 \\ -u_4 + u_5 &= 0 \\ -u_{2N+r+1} + u_{2N+r+2} &= 0. \end{aligned} \tag{6.24}$$

A ghost point was added to the right boundary since x_{2N+r+2} is outside of the domain.

Example: Let $N = 5$ then $h = \frac{1}{5} = 0.2$, $\delta = 0.6$, and the domain is discretized as follows.

Boundary Regions: $\{x_1, x_2, x_3, x_4, x_{14}\} = \{-1.6, -1.4, -1.2, -1, 1\}$

Nonlocal Region: $\{x_5, x_6, x_7, x_8\} = \{-0.8, -0.6, -0.4, -0.2\}$

Transtional Region $\{x_9, x_{10}, x_{11}\} = \{0, 0.2, 0.4\}$

Local Region $\{x_{12}, x_{13}\} = \{0.6, 0.8\}$

Ghost Point $\{x_{15}\} = \{1.2\}$

Exact Solution: $u(x,t) = (1-x^2)^2 e^{-t}$

Force Function: $u_t = u_{xx} + f \implies f = u_t - u_{xx} = -(1-x^2)e^{-t} - 4e^{-t}(3x^2 - 1)$

$$
\begin{bmatrix}
-1 & 1 & 0 & 0 & 0 & 0 & 0 & 0 & 0 & 0 & 0 & 0 & 0 & 0 & 0 \\
0 & -1 & 1 & 0 & 0 & 0 & 0 & 0 & 0 & 0 & 0 & 0 & 0 & 0 & 0 \\
0 & 0 & -1 & 1 & 0 & 0 & 0 & 0 & 0 & 0 & 0 & 0 & 0 & 0 & 0 \\
0 & 0 & 0 & -1 & 1 & 0 & 0 & 0 & 0 & 0 & 0 & 0 & 0 & 0 & 0 \\
0 & NL & NL & NL & NL & NL & NL & NL & 0 & 0 & 0 & 0 & 0 & 0 & 0 \\
0 & 0 & NL & NL & NL & NL & NL & NL & NL & 0 & 0 & 0 & 0 & 0 & 0 \\
0 & 0 & 0 & NL & NL & NL & NL & NL & NL & NL & 0 & 0 & 0 & 0 & 0 \\
0 & 0 & 0 & 0 & NL & NL & NL & NL & NL & NL & NL & 0 & 0 & 0 & 0 \\
0 & 0 & 0 & 0 & 0 & 0 & T & T & T & T & T & 0 & 0 & 0 & 0 \\
0 & 0 & 0 & 0 & 0 & 0 & 0 & T & T & T & T & T & 0 & 0 & 0 \\
0 & 0 & 0 & 0 & 0 & 0 & 0 & 0 & T & T & T & T & T & 0 & 0 \\
0 & 0 & 0 & 0 & 0 & 0 & 0 & 0 & 0 & 0 & L & L & L & 0 & 0 \\
0 & 0 & 0 & 0 & 0 & 0 & 0 & 0 & 0 & 0 & 0 & L & L & L & 0 \\
0 & 0 & 0 & 0 & 0 & 0 & 0 & 0 & 0 & 0 & 0 & 0 & -1 & 1 & 0 \\
0 & 0 & 0 & 0 & 0 & 0 & 0 & 0 & 0 & 0 & 0 & 0 & 0 & -1 & 1
\end{bmatrix}
\cdot
\begin{bmatrix} u_1 \\ u_2 \\ u_3 \\ u_4 \\ u_5 \\ u_6 \\ u_7 \\ u_8 \\ u_9 \\ u_{10} \\ u_{11} \\ u_{12} \\ u_{13} \\ u_{14} \\ u_{15} \end{bmatrix}
=
\begin{bmatrix} f_1 \\ f_2 \\ f_3 \\ f_4 \\ f_5 \\ f_6 \\ f_7 \\ f_8 \\ f_9 \\ f_{10} \\ f_{11} \\ f_{12} \\ f_{13} \\ f_{14} \\ f_{15} \end{bmatrix}
$$

Numerical Example: Let $N = 800$.

Exact Solution: $u(x,t) = (1-x^2)^2 e^{-t}$

Force Function: $u_t = u_{xx} + f$, so $f = u_t - u_{xx} = -(1-x^2)e^{-t} - 4e^{-t}(3x^2-1)$

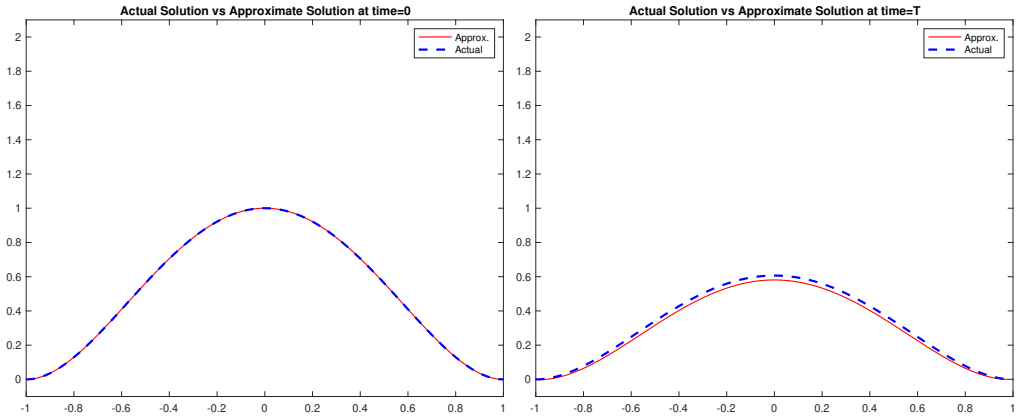

(a) solutions at $t = 0$ (b) solutions at $t = 1$

Figure 6.1: Numerical comparison between approximate and actual solution with Neumann Boundary Conditions

Convergence with respect to Δx is observed. The convergence order and $L^{\infty}_{\Omega\times[0,T]}$ differences between $u^{\ell}(x,t)$ and discrete solution of $u^{qnl}_{\delta,\Delta x}$ are listed in Table 6.1. Also the visual comparison of the two solutions at $t = 0$ and $t = T$ are displayed in Figure 6.1 with good agreement.

Table 6.1: $L^{\infty}_{\Omega\times[0,T]}$ differences between the local continuous solution u^{ℓ} and discrete solution $u^{qnl}_{\delta,\Delta x}$. We fix $\delta = 3\Delta x$, and the kernel is $\gamma_{\delta}(s) = \frac{3}{\delta^3}\chi_{[-\delta,\delta]}(s)$. The termination time $T = 1$ and $\Delta t = 0.2\Delta x$.

Δx	$\|\|u^{\ell}(x_i,t^n) - u^{qnl}_{\delta,\Delta x}(x_i,t^n)\|\|_{L^{\infty}_{\Omega\times[0,T]}}$	Order
$\frac{1}{50}$	0.043475181041249	–
$\frac{1}{100}$	0.030146283494951	0.528211881043193
$\frac{1}{200}$	0.027006777957941	0.158658624768605
$\frac{1}{400}$	0.026252384772113	0.040873046015994
$\frac{1}{800}$	0.026073056145894	0.009888785574533
$\frac{1}{1600}$	0.026032317516913	0.002255945053181

6.3 Coefficient Matrix with Robin Boundary Conditions and Numerical Example

Next we repeat the same process with the same constraints for the LNL Robin Boundary Condition Problem

$$\begin{cases} u_t(x,t) = \mathcal{L}^{qnl}u(x,t) + f(x,t) & x \in [-1,1] \\ u(x,0) = u_0(x) & x \in (-1,1) \\ u_x(x,t) - u(x,t) = 0 & x \in [-\delta - 1, -1] \cup \{1\} \end{cases}$$

This time the Robin Boundary Conditions and definition of $u_x(x,t)$ gives

$$u_x(x_1,t) - u(x_1,t) = 0 \tag{6.25}$$

which implies

$$u(x_2,t) - u(x_1,t)h - u(x_1,t) = 0, \quad \text{or} \quad \frac{(-1-h)}{h}u_1 + u_2 = 0. \tag{6.26}$$

Similarly

$$\begin{aligned} &\frac{(-1-h)}{h}u_2 + u_3 = 0 \\ &\frac{(-1-h)}{h}u_3 + u_4 = 0 \\ &\frac{(-1-h)}{h}u_4 + u_5 = 0 \\ &\frac{(-1-h)}{h}u_{14} + u_{15} = 0. \end{aligned} \tag{6.27}$$

Again a ghost point was needed at the right boundary since x_{15} is outside of the specified domain.

Example: Let $N = 5$ then $h = \frac{1}{5} = 0.2$, $\delta = 0.6$, and the domain is discretized as follows.

Boundary Regions: $\{x_1, x_2, x_3, x_4, x_{14}\} = \{-1.6, -1.4, -1.2, -1, 1\}$

Nonlocal Region: $\{x_5, x_6, x_7, x_8\} = \{-0.8, -0.6, -0.4, -0.2\}$

Transtional Region $\{x_9, x_{10}, x_{11}\} = \{0, 0.2, 0.4\}$

Local Region $\{x_{12}, x_{13}\} = \{0.6, 0.8\}$

Ghost Point $\{x_{15}\} = \{1.2\}$

$$\begin{bmatrix}
\frac{-1-h}{h} & 1 & 0 & 0 & 0 & 0 & 0 & 0 & 0 & 0 & 0 & 0 & 0 & 0 & 0 \\
0 & \frac{-1-h}{h} & 1 & 0 & 0 & 0 & 0 & 0 & 0 & 0 & 0 & 0 & 0 & 0 & 0 \\
0 & 0 & \frac{-1-h}{h} & 1 & 0 & 0 & 0 & 0 & 0 & 0 & 0 & 0 & 0 & 0 & 0 \\
0 & 0 & 0 & \frac{-1-h}{h} & 1 & 0 & 0 & 0 & 0 & 0 & 0 & 0 & 0 & 0 & 0 \\
0 & NL & NL & NL & NL & NL & NL & NL & 0 & 0 & 0 & 0 & 0 & 0 & 0 \\
0 & 0 & NL & NL & NL & NL & NL & NL & NL & 0 & 0 & 0 & 0 & 0 & 0 \\
0 & 0 & 0 & NL & NL & NL & NL & NL & NL & NL & 0 & 0 & 0 & 0 & 0 \\
0 & 0 & 0 & 0 & NL & NL & NL & NL & NL & NL & NL & 0 & 0 & 0 & 0 \\
0 & 0 & 0 & 0 & 0 & 0 & T & T & T & T & T & 0 & 0 & 0 & 0 \\
0 & 0 & 0 & 0 & 0 & 0 & 0 & T & T & T & T & T & 0 & 0 & 0 \\
0 & 0 & 0 & 0 & 0 & 0 & 0 & 0 & T & T & T & T & T & 0 & 0 \\
0 & 0 & 0 & 0 & 0 & 0 & 0 & 0 & 0 & 0 & L & L & L & 0 & 0 \\
0 & 0 & 0 & 0 & 0 & 0 & 0 & 0 & 0 & 0 & 0 & L & L & L & 0 \\
0 & 0 & 0 & 0 & 0 & 0 & 0 & 0 & 0 & 0 & 0 & 0 & \frac{-1-h}{h} & 1 & 0 \\
0 & 0 & 0 & 0 & 0 & 0 & 0 & 0 & 0 & 0 & 0 & 0 & 0 & \frac{-1-h}{h} & 1
\end{bmatrix} \cdot \begin{bmatrix} u_1 \\ u_2 \\ u_3 \\ u_4 \\ u_5 \\ u_6 \\ u_7 \\ u_8 \\ u_9 \\ u_{10} \\ u_{11} \\ u_{12} \\ u_{13} \\ u_{14} \\ u_{15} \end{bmatrix} = \begin{bmatrix} f_1 \\ f_2 \\ f_3 \\ f_4 \\ f_5 \\ f_6 \\ f_7 \\ f_8 \\ f_9 \\ f_{10} \\ f_{11} \\ f_{12} \\ f_{13} \\ f_{14} \\ f_{15} \end{bmatrix}$$

Numerical Example: Let $N = 800$.

Exact Solution: $u(x,t) = (1-x^2)^2 e^{-t}$

Force Function: $u_t = u_{xx} + f$, so $f = u_t - u_{xx} = -(1-x^2)e^{-t} - 4e^{-t}(3x^2-1)$

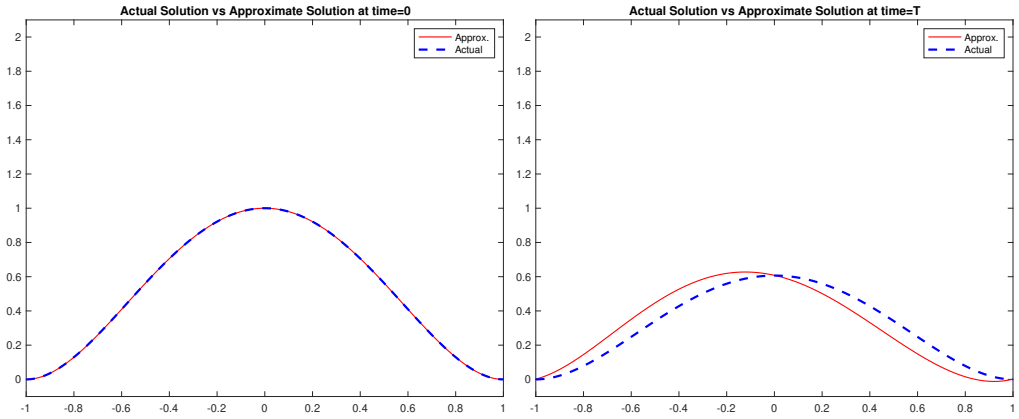

(a) solutions at $t = 0$ (b) solutions at $t = 1$

Figure 6.2: Numerical comparison between approximate and actual solution with Robin Boundary Conditions

Convergence with respect to Δx is observed. The convergence order and $L^{\infty}_{\Omega\times[0,T]}$ differences between $u^{\ell}(x,t)$ and discrete solution of $u^{qnl}_{\delta,\Delta x}$ are listed in Table 6.2. Also the visual comparison of the two solutions at $t = 0$ and $t = T$ are displayed in Figure 6.2 with good agreement.

Table 6.2: $L^{\infty}_{\Omega\times[0,T]}$ differences between the local continuous solution u^{ℓ} and discrete solution $u^{qnl}_{\delta,\Delta x}$. We fix $\delta = 3\Delta x$, and the kernel is $\gamma_{\delta}(s) = \frac{3}{\delta^3}\chi_{[-\delta,\delta]}(s)$. The termination time $T = 1$ and $\Delta t = 0.2\Delta x$.

Δx	$\|\|u^{\ell}(x_i,t^n) - u^{qnl}_{\delta,\Delta x}(x_i,t^n)\|\|_{L^{\infty}_{\Omega\times[0,T]}}$	Order
$\frac{1}{50}$	0.122782280120421	–
$\frac{1}{100}$	0.125558097493344	−0.032252707227395
$\frac{1}{200}$	0.124303728858722	0.014485498951618
$\frac{1}{400}$	0.122898978578868	0.016396649521443
$\frac{1}{800}$	0.121986716387248	0.010748869820472
$\frac{1}{1600}$	0.121475868914773	0.006054303546220

6.4 Boundary Conditions Conclusion

The results from numerical examples with Dirichlet, Neumann, and Robin boundary conditions paint a very clear picture. The best results are found with models that have Dirichlet boundary conditions. Applying the LNL finite difference scheme with either Neumann or Robin boundary conditions fail to produce as accurate an approximation with strong convergence. The result for the example with Robin boundary conditions was also much weaker than the result from the example with Neumann boundary conditions. This is due to the lack of symmetry of a solution with Robin boundary conditions, which would then alter the continuous operator derived from energy variation. This could lead to future work altering the continuous model to apply to non symmetric solutions, allowing for better approximations of solutions with Robin boundary conditions. We still applied the finite difference scheme to approximate a solution with Robin boundary conditions to compare results.

REFERENCES

[1] Burak Aksoylu and Michael L. Parks. Variational theory and domain decomposition for nonlocal problems. *Applied Mathematics and Computation*, 217(14):6498–6515, 2011.

[2] Fuensanta Andreu-Vaillo, Jose M. Mazon, Julio D. Rossi, and J.Julian Toledo-Melero. *Nonlocal diffusion problems*. Mathematical surveys and monographs ; v. 165. American Mathematical Society, Providence, R.I, 2010.

[3] P. Bates and A. Chmaj. An integrodifferential model for phase transitions: Stationary solutions in higher space dimensions. *Journal of Statistical Physics*, 95:1119–1139, 1999.

[4] F. Bobaru and M. Duangpanya. The peridynamic formulation for transient heat conduction. *International Journal of Heat and Mass Transfer*, 53:4047–4059, 2010.

[5] Floran Bobaru and Monchai Duangpanya. The peridynamic formulation for transient heat conduction. *International Journal of Heat and Mass Transfer*, 53(19):4047–4059, 2010.

[6] Allert Bruckmaier F, Neuling R, Littin N, Amrein P, and Briegel K S. Imaging local diffusion in microstructures using nv-based pulsed field gradient nmr. In *Cambridge: Cambridge Open Engage*, volume preprint, 2023.

[7] A. Buades, B. Coll, and J. M. Morel. Image denoising methods. a new nonlocal principle. *SIAM Review*, 52(1):113–147, 2010.

[8] Claudia Bucur and Enrico Valdinoci. *Nonlocal diffusion and applications*. Springer, 2016.

[9] Ceren Budak, Divyakant Agrawal, and Amr El Abbadi. Diffusion of information in social networks: Is it all local? In *2012 IEEE 12th International Conference on Data Mining*, pages 121–130, 2012.

[10] Emmanuel Chasseigne, Manuela Chaves, and Julio D. Rossi. Asymptotic behavior for nonlocal diffusion equations. *Journal de Mathematiques Pures et Appliquees*, 86:271–291, 2006.

[11] Marta D'Elia, Xingjie Li, Pablo Seleson, Xiaochuan Tian, and Yue Yu. A review of local-to-nonlocal coupling methods in nonlocal diffusion and nonlocal mechanics. *To appear on Journal of Peridynamics and Nonlocal Modeling*, 2020.

[12] Qiang Du, Max Gunzburger, R Lehoucq, and Kun Zhou. Analysis and approximation of nonlocal diffusion problems with volume constraints. *SIAM Review*, 56:676–696, 2012.

[13] Qiang Du, Max Gunzburger, R Lehoucq, and Kun Zhou. A nonlocal vector calculus, nonlocal volume-constrained problems, and nonlocal balance laws. *Mathematical Models and Methods in Applied Sciences*, 23:493–540, 2013.

[14] Qiang Du, Xingjie Helen Li, Jianfeng Lu, and Xiaochuan Tian. A quasinonlocal coupling method for nonlocal and local diffusion models. *SIAM Journal on Numerical Analysis*, 56:1386–1404, 2018.

[15] Qiang Du and Robert Lipton. Peridynamics, fracture, and nonlocal continuum models. *SIAM News*, 47(3), 2014.

[16] Qiang Du and Kun Zhou. Mathematical analysis for the peridynamic nonlocal continuum theory. *Mathematical Modelling and Numerical Analysis*, 45:217–234, 2010.

[17] Marta DâElia, Qiang Du, Christian Glusa, Max Gunzburger, Xiaochuan Tian, and Zhi Zhou. Numerical methods for nonlocal and fractional models. *Acta Numerica*, 29:1–124, 2020.

[18] M. Elices, G. V. Guinea, J. GÃ^3$mez, and J. Planas. The cohesive zone model : advantages, limitations and challenges. Engineering Fracture Mechanics, 69 : 137 − −163, 2002.

[19] Paul Fife. Some nonclassical trends in parabolic and parabolic-like evolutions. In *Trends in Nonlinear Analysis*, pages 153–191. Springer, 2003.

[20] Walter Gerstle, Nicolas Sau, and Stewart Silling. Peridynamic modeling of plain and reinforced concrete structures. *18th International Conference on Structural Mechanics in Reactor Technology (SMiRT 18)*, 2005.

[21] Guy Gilboa and Stanley Osher. Nonlocal operators with applications to image processing. *Multiscale Modeling and Simulation*, 7(3):1005–1028, 2009.

[22] Amanda Gute and Xingjie Li. Maximum principle preserving finite difference scheme for 1-d nonlocal-to-local diffusion problems. *Results in Applied Mathematics*, 12, 2021.

[23] Y. D. Ha and F. Bobaru. Studies of dynamic crack propagation and crack branching with peridynamics. *International Journal of Fracture*, 162:229–244, 2010.

[24] Y. D. Ha and F. Bobaru. Characteristics of dynamic brittle fracture captured with peridynamics. *Engineering Fracture Mechanics*, 78:1156–1168, 2011.

[25] Siavash Jafarzadeh and Adam Larios. Efficient solutions for nonlocal diffusion problems boundary-adapted spectral methods. *Journal of Peridynamics and Nonlocal Modeling*, 2:85–110, 2020.

[26] Dennis Kriventsov. Regularity for a local-nonlocal transmission problem. *Archive for Rational Mechanics and Analysis*, 217, 04 2014.

[27] Xingjie Helen Li and Jianfeng Lu. Quasinonlocal coupling of nonlocal diffusions. *SIAM*, 2016. arXiv preprint arXiv:1607.03940.

[28] Xingjie Helen Li and Jianfeng Lu. Quasi-nonlocal coupling of nonlocal diffusions. *SIAM Journal on Numerical Analysis*, 55(5):2394–2415, 2017.

[29] Xingjie Helen Li and Jianfeng Lu. Quasinonlocal coupling of nonlocal diffusions. *SIAM*, 55, 2017.

[30] Xingjie Helen Li and Mitchell Luskin. A generalized quasinonlocal atomistic-to-continuum coupling method with finite-range interaction. *IMA Journal of Numerical Analysis*, 32:373–393, 2011.

[31] R. Lipton. Dynamic brittle fracture as a small horizon limit of peridynamics. *Journal of Elasticity*, 117:21–50, 2014.

[32] R. Lipton. Cohesive dynamics and brittle fracture. *Journal of Elasticity*, 124:143–191, 2016.

[33] Q. Ma, W. Li, J. Bortnik, R. M. Thorne, X. Chu, L. G. Ozeke, G. D. Reeves, C. A. Kletzing, W. S. Kurth, G. B. Hospodarsky, M. J. Engebretson, H. E. Spence, D. N. Baker, J. B. Blake, J. F. Fennell, and S. G. Claudepierre. Quantitative evaluation of radial diffusion and local acceleration processes during gem challenge events. *Journal of Geophysical Research: Space Physics*, 123(3):1938–1952, 2018.

[34] Eduard Marusic-Paloka and Igor Pazanin. The robin boundary condition for modeling heat transfer. *Proceedings of the Royal Society A*, 480, 2024.

[35] M. L. Parks, Richard B. Lehoucq, Steven J. Plimpton, and Stewart Silling. Implementing peridynamics within a molecular dynamics code. *Computer Physics Communications*, 179:777–783, 2008.

[36] Lorenzo Rosasco, Mikhail Belkin, and Ernesto De Vito. On learning with integral operators. *Journal of Machine Learning Research*, 11(30):905–934, 2010.

[37] Julio Rossi. Nonlocal diffusion equations with integrable kernels. *Notices of the American Mathematical Society*, September 2020.

[38] H. L. Royden. *Real analysis [by] H. L. Royden.* Macmillan, New York, 2d ed. edition, 1968.

[39] S.A. Silling and R.B.Lehoucq. Peridynamic theory of solid mechanics. *ScienceDirect*, 44:73–168, 2010.

[40] Stewart Silling. Reformulation of elasticity theory for discontinuities and long-range forces. *Journal of the Mechanics and Physics of Solids*, 48:175–209, 2000.

[41] Stewart Silling and R. B. Lehoucq. Peridynamic theory of solid mechanics. *Advances in Applied Mechanics*, 44:73–168, 2010.

[42] Michael J. Steele. *Stochastic calculus and financial applications.* Springer, 2010.

[43] Xiaochuan Tian and Qiang Du. Analysis and comparison of different approximations to nonlocal diffusion and linear peridynamic equations. *SIAM Journal on Numerical Analysis*, 51:3458–3482, 2013.

[44] Xiaochuan Tian and Qiang Du. Asymptotically compatible schemes and applications to robust discretization of nonlocal models. *SIAM Journal on Numerical Analysis*, 52:1641–1665, 2014.

[45] N. Trask, H. You, Y. Yu, and M. L. Parks. An asymptotically compatible meshfree quadrature rule for nonlocal problems with applications to peridynamics. *Computer Methods in Applied Mechanics and Engineering*, 343:151–165, 2019.

[46] Jan TÃžnnesen, Sabina HrabÄtovÃ¡, and Federico N. Soria. Local diffusion in the extracellular space of the brain. *Neurobiology of Disease*, 177:105981, 2023.

[47] M. Vynnycky. An asymptotic model for the formation and evolution of air gaps in vertical continuous casting. *Proceedings of the Royal Society A*, 465, 2009.

[48] H. You, Y. Yu, and D. Kamensky. An asymptotically compatible formulation for local-to-nonlocal coupling problems without overlapping regions. *Computer Methods in Applied Mechanics and Engineering*, 366, 2020.